

**QUALITATIVE AND QUANTITATIVE ASSESSMENT
OF HEMODYNAMIC PARAMETERS BY 4D FLOW
MRI IN UNCOMPLICATED DESCENDING (TYPE B)
AORTIC DISSECTION.**

DR. BELLALA AJAY PAVAN KUMAR

**DM CARDIOVASCULAR IMAGING AND VASCULAR INTERVENTIONAL
RADIOLOGY**

(2020-2022)



**SREE CHITRA TIRUNAL INSTITUTE FOR MEDICAL SCIENCES AND
TECHNOLOGY, TRIVANDRUM**

An Institution of National Importance established by an Act of the Indian Parliament

(Act No.52 of 1980)

Dept. of Science and Technology, Govt. of India

www.sctimst.ac.in



**QUALITATIVE AND QUANTITATIVE ASSESSMENT OF
HEMODYNAMIC PARAMETERS BY 4D FLOW MRI IN
UNCOMPLICATED DESCENDING (TYPE B) AORTIC DISSECTION.**

A THESIS SUBMITTED BY

DR. BELLALA AJAY PAVAN KUMAR

TO

SREE CHITRA TIRUNAL INSTITUTE FOR MEDICAL SCIENCES AND
TECHNOLOGY, TRIVANDRUM.

IN PARTIAL FULFILMENT OF THE REQUIREMENTS

FOR THE AWARD OF

**DM CARDIOVASCULAR IMAGING AND VASCULAR INTERVENTIONAL
RADIOLOGY**

(2020-2022)

DECLARATION BY THE STUDENT

CERTIFICATE

I, Dr. Bellala Ajay Pavan Kumar hereby certify that I had personally carried out the work depicted in the thesis titled, “**Qualitative and quantitative assessment of hemodynamic parameters by 4D flow MRI in uncomplicated descending (type B) aortic dissection.**”

No part of this thesis has been submitted for the award of any other degree or diploma prior to this date.

Signature



Name of the Candidate

Bellala. Ajay Pavan Kumar

Date: 13-8-2022

(* If external help was sought, declare and acknowledge)

CERTIFICATE BY THE RESEARCH GUIDE



श्री चित्रा तिरुनाल आयुर्विज्ञान और प्रौद्योगिकी संस्थान, त्रिवेन्द्रम
तिरुवनन्तपुरम - ६९५०११, केरल, इंडिया
SREE CHITRA TIRUNAL INSTITUTE FOR MEDICAL SCIENCES AND TECHNOLOGY, TRIVANDRUM
Thiruvananthapuram - 695 011, Kerala, India
(An Institute of National Importance under Govt. of India)

Grams : Chitramet, Phone : +91-471-2443152, Fax : +91-471-2550728 / 2446433, E-mail : sct@sctimst.ac.in, Website : www.sctimst.ac.in

Name of the Guide: *Jineesh Valakkada*

Division/Department: **Dept of Imaging Sciences & Interventional Radiology**

This is to certify that Dr. Bellala. Ajay Pavan Kumar, department of **Imaging Sciences & Interventional Radiology** of this institute has fulfilled the requirements prescribed for the **DM Cardiovascular Imaging and Vascular Interventional Radiology** degree of the Sree Chitra Tirunal Institute for Medical Sciences and Technology, Trivandrum.

The thesis entitled, "**Qualitative and quantitative assessment of hemodynamic parameters by 4D flow MRI in uncomplicated descending (type B) aortic dissection.**" was carried out under my direct supervision. No part of the thesis was submitted for the award of any degree or diploma prior to this date.

*Clearance was obtained from the Institutional Ethics Committee / Institutional Animal Ethics / Institutional Committee for Stem Cell Research / Other appropriate committees (if any, specify) for carrying out the study.

Signature
Name of the Guide

Date

*As and when applicable. If an external co-guide was present, a similar declaration should be made, provided a substantial part of the thesis work was done under co-guide.

CERTIFICATE BY THE RESEARCH CO-GUIDE

(*in institute letterhead)



श्री चित्रा तिरुनाल आयुर्विज्ञान और प्रौद्योगिकी संस्थान, त्रिवेन्द्रम
तिरुवनन्तपुरम - ६९५०११, केरल, इंडिया
SREE CHITRA TIRUNAL INSTITUTE FOR MEDICAL SCIENCES AND TECHNOLOGY, TRIVANDRUM
Thiruvananthapuram - 695 011, Kerala, India
(An Institute of National Importance under Govt. of India)

Grams Chitramet, Phone : +91-471-2443152, Fax : +91-471-2550728 / 2446433, E-mail : scl@sctimst.ac.in, Website : www.sctimst.ac.in

Name of the Co-Guide: *Dr. Anoop Ayyappan*

Division/Department: **Dept of Imaging Sciences & Interventional Radiology**

This is to certify that Dr. Bellala. Ajay Pavan Kumar, department of **Imaging Sciences & Interventional Radiology** of this institute has fulfilled the requirements prescribed for the DM *Cardiovascular Imaging and Vascular Interventional Radiology* degree of the Sree Chitra Tirunal Institute for Medical Sciences and Technology, Trivandrum.

The thesis entitled, "**Qualitative and quantitative assessment of hemodynamic parameters by 4D flow MRI in uncomplicated descending (type B) aortic dissection.**" was carried out under my direct supervision. No part of the thesis was submitted for the award of any degree or diploma prior to this date.

*Clearance was obtained from the Institutional Ethics Committee / Institutional Animal Ethics / Institutional Committee for Stem Cell Research / Other appropriate committees (if any, specify) for carrying out the study.

Signature
Name of the Co-Guide
Dr. Anoop

Date *15/8/2022*

*As and when applicable. If an external co-guide was present, a similar declaration should be made, provided a substantial part of the thesis work was done under co-guide.

CERTIFICATE BY THE RESEARCH GUIDE

(*in institute letterhead)



श्री चित्रा तिरुनाल आयुर्विज्ञान और प्रौद्योगिकी संस्थान, त्रिवेन्द्रम
तिरुवनन्तपुरम - ६९५०११, केरल, इंडिया
SREE CHITRA TIRUNAL INSTITUTE FOR MEDICAL SCIENCES AND TECHNOLOGY, TRIVANDRUM
Thiruvananthapuram - 695 011, Kerala, India
(An Institute of National Importance under Govt. of India)

Grams : Chitramet, Phone : +91-471-2443152, Fax : +91-471-2550728 / 2446433, E-mail : sct@sctimst.ac.in, Website : www.sctimst.ac.in

Name of the Co-Guide: *Dr. Santhosh Kumar K.*

Division/Department: **Dept of Imaging Sciences & Interventional Radiology**

This is to certify that Dr. Bellala. Ajay Pavan Kumar, department of **Imaging Sciences & Interventional Radiology** of this institute has fulfilled the requirements prescribed for the DM *Cardiovascular Imaging and Vascular Interventional Radiology* degree of the Sree Chitra Tirunal Institute for Medical Sciences and Technology, Trivandrum.

The thesis entitled, "**Qualitative and quantitative assessment of hemodynamic parameters by 4D flow MRI in uncomplicated descending (type B) aortic dissection.**" was carried out under my direct supervision. No part of the thesis was submitted for the award of any degree or diploma prior to this date.

*Clearance was obtained from the Institutional Ethics Committee / Institutional Animal Ethics / Institutional Committee for Stem Cell Research / Other appropriate committees (if any, specify) for carrying out the study.

Signature

Name of the Co-Guide

Dr. Santhosh Kumar K

Date *11.08.2022*

*As and when applicable. If an external co-guide was present, a similar declaration should be made, provided a substantial part of the thesis work was done under co-guide.

CERTIFICATE BY THE RESEARCH CO-GUIDE

(*in institute letterhead)



श्री चित्रा तिरुनाल आयुर्विज्ञान और प्रौद्योगिकी संस्थान, त्रिवेन्द्रम
तिरुवनन्तपुरम - ६९५०११, केरल, इंडिया
SREE CHITRA TIRUNAL INSTITUTE FOR MEDICAL SCIENCES AND TECHNOLOGY, TRIVANDRUM
Thiruvananthapuram - 695 011, Kerala, India
(An Institute of National Importance under Govt. of India)

Grams : Chitramet, Phone : +91-471-2443152, Fax : +91-471-2550728 / 2446433, E-mail : sct@sctimst.ac.in, Website : www.sctimst.ac.in

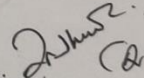
Name of the Co-Guide: *Dr. Shivanesan. P*

Division/Department: **Dept of Cardiovascular and Thoracic surgery**

This is to certify that Dr. Bellala. Ajay Pavan Kumar, department of **Imaging Sciences & Interventional Radiology** of this institute has fulfilled the requirements prescribed for the DM *Cardiovascular Imaging and Vascular Interventional Radiology* degree of the Sree Chitra Tirunal Institute for Medical Sciences and Technology, Trivandrum.

The thesis entitled, "**Qualitative and quantitative assessment of hemodynamic parameters by 4D flow MRI in uncomplicated descending (type B) aortic dissection.**" was carried out under my direct supervision. No part of the thesis was submitted for the award of any degree or diploma prior to this date.

*Clearance was obtained from the Institutional Ethics Committee / Institutional Animal Ethics / Institutional Committee for Stem Cell Research / Other appropriate committees (if any, specify) for carrying out the study.


Signature (Dr. P. SHIVANEJAN)
Name of the Co-Guide

Date *11/08/2022*

*As and when applicable. If an external co-guide was present, a similar declaration should be made, provided a substantial part of the thesis work was done under co-guide.

APPROVAL OF THE THESIS



श्री चित्रा तिरुनाल आयुर्विज्ञान और प्रौद्योगिकी संस्थान, त्रिवेन्द्रम
तिरुवनन्तपुरम - ६९५०११, केरल, इंडिया
SREE CHITRA TIRUNAL INSTITUTE FOR MEDICAL SCIENCES AND TECHNOLOGY, TRIVANDRUM
Thiruvananthapuram - 695 011, Kerala, India
(An Institute of National Importance under Govt. of India)

Grams : Chitramet, Phone : +91-471-2443152, Fax : +91-471-2550728 / 2446433, E-mail : scl@sctimst.ac.in, Website : www.sctimst.ac.in

APPROVAL OF THE THESIS

The thesis entitled

**Qualitative and quantitative assessment of hemodynamic parameters by 4D flow
MRI in uncomplicated descending aortic(type B) dissection**

Submitted by

Dr. Bellala. Ajay Pavan Kumar

for the degree of

**DM CARDIOVASCULAR IMAGING AND VASCULAR INTERVENTIONAL
RADIOLOGY**

of

SREE CHITRA TIRUNAL INSTITUTE FOR MEDICAL SCIENCES AND
TECHNOLOGY, TRIVANDRUM

is evaluated and approved by

Dr Jineesh Valakkada

(Name & Signature of the Guide)

(Name & Signature of thesis examiner)

APPROVAL OF THE THESIS

(in institute letterhead)

The thesis entitled

**Qualitative and quantitative assessment of hemodynamic parameters by
4D flow MRI in uncomplicated descending aortic(type B) dissection**

Submitted by

Dr. Bellala. Ajay Pavan Kumar

for the degree of

**DM CARDIOVASCULAR IMAGING AND VASCULAR
INTERVENTIONAL RADIOLOGY**

of

**SREE CHITRA TIRUNAL INSTITUTE FOR MEDICAL SCIENCES AND
TECHNOLOGY, TRIVANDRUM**

is evaluated and approved by

Dr Jineesh Valakkada

.....

(Name & Signature of the
Guide)

(Name & Signature of thesis
examiner)

ACKNOWLEDGEMENTS

- ✦ I hereby express my sincere gratitude to all my teachers & guides especially Dr Jineesh Valakkada (Associate Professor), Dr. Anoop Ayyappan (Associate Professor), Dr Santhosh Kumar (Additional Professor), Department of Imaging Sciences and Interventional Radiology, Dr. Shivanesan.P. (Associate Professor), Department of cardiovascular and thoracic surgery for their constant unwavering support, insightful criticism, expert supervision and immense patience throughout this study.
- ✦ I would specially like to acknowledge my gratitude to my past and present colleagues and the technologists of the Department of IS and IR and the advanced radiology technology trainees of the department for their valuable assistance at all times during this study.
- ✦ I would also like to extend my heartfelt gratitude to my family for being immensely supportive all through my endeavours. I could not have achieved what I have without their prayers, love and support.
- ✦ Last but not least I am eternally grateful to all my patients & their relatives who have been very understanding and generous with their cooperation all through the study.



TABLE OF CONTENTS

DECLARATION BY THE STUDENT	i
CERTIFICATE BY THE RESEARCH GUIDE	Error! Bookmark not defined.
(*in institute letterhead)	Error! Bookmark not defined.
CERTIFICATE BY THE RESEARCH CO-GUIDE	ii
(*in institute letterhead)	iii
CERTIFICATE BY THE RESEARCH GUIDE	iv
(*in institute letterhead)	iv
CERTIFICATE BY THE RESEARCH CO-GUIDE	iv
(*in institute letterhead)	v
ACKNOWLEDGEMENTS	viii
TABLE OF CONTENTS	x
LIST OF FIGURES	xi
LIST OF TABLES	xiv
LIST OF ABBREVIATIONS (Optional)	xvi
SYNOPSIS	xix
1 INTRODUCTION	21
2 LITERATURE REVIEW	24
3 MATERIALS AND METHODS	43
4 RESULTS	55
.....	62
5 DISCUSSION	95
6 SUMMARY AND CONCLUSIONS	104
7 REFERENCES	106
ANNEXURES	110

LIST OF FIGURES

Figure No	Figure Caption	Page No
Figure 1	Stanford and DeBakey Classification	26
Figure 2	basic acquisition of 4D flow	34
Figure 3	Flow chart showing flow design	45
Figure 4	Anatomical measurements from CT angiography	47
Figure 5	SVS/STS standards for measurement of TL, FL, Aorta sizes in AD	48
Figure 6	Flow chart showing basic steps in 4D flow	49
Figure 7	Image showing initial processing step and segmentation of aorta	50
Figure 8	Image showing technique of measuring flow volumes and velocities across vessel	51
Figure 9	Technique for calculation of energy loss and WSS	53
Figure 10	Flow chart of the results	56
Figure 11	Scatter plot showing analysis of demographic, morphological parameter	62
Figure 12	Scatter plot showing relationship between growth rate and various morphological parameters	65
Figure 13	Scatter plot showing correlation between growth rate and False lumen ejection fraction	67

Figure 14	Scatter plot showing correlation between growth rate and energy loss in the DTA	68
Figure 15	Scatter plot showing correlation between growth rate and percentage energy loss in the DTA	70
Figure 16	Scatter plot showing correlation between growth rate and circumferential wall shear stress of false lumen	72
Figure 17	Scatter plot showing correlation between growth rate and circumferential wall shear stress of true lumen	74
Figure 18	Scatter plot showing correlation between growth rate and wall shear stress of ascending aorta	75
Figure 19	Scatter plot showing correlation between growth rate and axial wall shear stress of true lumen	77
Figure 20	Scatter plot showing correlation between growth rate and axial wall shear stress of false lumen	78
Figure 21	Scatter plot showing correlation between growth rate and peak systolic velocity of false lumen	80
Figure 22	Scatter plot showing correlation between growth rate and peak systolic velocity of true lumen	81
Figure 23	Bland Altman plot for PSV of true lumen between observer 1 and 2	84

Figure 24	Bland Altman plot for PSV of false lumen between observer 1 and 2	85
Figure 25	Bland Altman plot for FLRF between observer 1 and 2	86
Figure 26	4D flow MRI images in a normal adult	87
Figure 27	Case of rapid expanding aorta in Type B AD patient	88
Figure 28	Case of rapidly expanding aorta in TBAD	89
Figure 29	Patient with TBAD having stable growth	90
Figure 30	Case of TBAD with stable growth	92
Figure 31	Flow patterns in 3 different patients	94

LIST OF TABLES

Table 1 Complicated, high risk and uncomplicated TBAD.....	28
Table 2 Morphological high-risk features which can result in rapid aortic growth	32
Table 3 Studies related to 4D flow MRI in aortic dissection was summarized in the following table.....	39
Table 4 Showing demographic details	57
Table 5 anatomic detail in initial scan.....	58
Table 6 Entry tear characteristics.....	59
Table 7 False lumen (FL) and true lumen(TL)characteristics	60
Table 8 Follow up details	61
Table 9 Statistical tests showing distribution of rate of expansion	62
Table 10 Demographic analysis.....	63
Table 11 Anatomical parameters analysis	64
Table 12 false lumen ejection fraction analysis	66
Table 13 Energy loss in the DTA analysis	67
Table 14 percentage of energy loss in the DTA analysis	69
Table 15 circumferential WSS of the FL(Pa) analysis	71
Table 16 circumferential WSS of the TL(Pa).....	73
Table 17 Max WSS of the ascending aorta (Pa) analysis.....	75
Table 18 Axial WSS of true lumen (Pa) analysis	76
Table 19 Axial WSS of False Lumen (Pa) analysis	77
Table 20 PSV in False lumen in proximal DTA.....	79
Table 21 PSV in True lumen in proximal DTA.....	80
Table 22 Multivariate analysis between various variables	82

Table 23 Interobserver variability related to PSV in TL	83
Table 24 Interobserver variability related to PSV in FL	84
Table 25 Interobserver variability related to false lumen ejection fraction	85



LIST OF ABBREVIATIONS (Optional)

S No	Abbreviation	Full Form
1	4D flow MRI	4-dimensional Magnetic Resonance Imaging
2	AD	aortic dissection
3	AP	Arterial phase
4	BPM	beats per minute
5	CFD	computational fluid dynamics
6	CKD	chronic kidney disease
7	CMR	cardiac MRI
8	Cir WSS	circumferential WSS
9	DP	delayed phase
10	EF	ejection fraction
11	EL	energy loss
12	FL	false lumen
13	FLRF	false lumen regurgitation fraction
14	FLEF	false lumen ejection fraction
15	MRI	Magnetic Resonance Imaging
16	NNT	number needed to treat
17	PSV	peak systolic velocity
18	Pa	Pascal
19	RF	regurgitant fraction

20	rTAAD	repaired type A aortic dissection
21	TBAD	Stanford type B aortic dissection
22	uTBAD	uncomplicated type B aortic dissection
23	TEVAR	thoracic endovascular aortic repair
24	TAWSS	Time averaged wall shear stress
25	TL	True lumen
26	WSS	Wall shear stress

SYNOPSIS

**QUALITATIVE AND QUANTITATIVE ASSESSMENT OF
HEMODYNAMIC PARAMETERS BY 4D FLOW MRI IN
UNCOMPLICATED DESCENDING (TYPE B) AORTIC DISSECTION.**

SYNOPSIS

BY

DR. BELLALA AJAY PAVAN KUMAR

for DM CARDIOVASCULAR IMAGING AND VASCULAR
INTERVENTIONAL RADIOLOGY

of

SREE CHITRA TIRUNAL INSTITUTE FOR MEDICAL SCIENCES AND
TECHNOLOGY, TRIVANDRUM

(The typed pages may be stapled and submitted three months prior to the
submission of the thesis. When synopsis forms part of the thesis, the cover page need
not be included)

SYNOPSIS

TITLE: Qualitative and quantitative assessment of hemodynamic parameters by 4D flow MRI in uncomplicated descending aortic (type B) dissection.

Aim:

- 1.To assess qualitative and quantitative flow parameters in uncomplicated descending aortic (type B) dissection by using 4D flow MRI.
- 2.To assess the relationship between the change in 4D flow parameters with the expansion of false lumen in type B aortic dissection.

Methods and Materials: A single-center prospective study was performed in 15 patients from 2020 to 2022 after obtaining informed consent. All patients underwent CT angiography and 4D flow MRI at the initial presentation and follow-up CT angiography after 1-2 years. Various 4D flow MR parameters including peak systolic velocity (PSV), regurgitation fraction (RF) in false lumen (FL) and true lumen (TL), wall shear strain (WSS) in the TL and FL, the percentage loss of energy in the DTA were measured in the cohort. The predictive values of these MR parameters for expansion (>3 mm/year) of aortic dissection were analyzed

Results: Among 15 cases, 5 patients showed enlarging aorta size of more than 3 mm in one year and 10 patients had stable aortic size (≤ 3 mm/year). Among the demographic and morphological parameters assessed, it is the entry tear size of more than 10 mm showed a medium, positive correlation with the growth rate with $r= 0.41$ and no significant association between the size of entry tear and the growth rate in millimeter, $r = 0.41$, $p = 0.131$. Other morphological and anatomical parameters did

not show difference between cases with stable size and enlarging aorta size. Among the 4D flow parameters, False lumen regurgitation fraction (FLRF) ($p=0.002$), energy loss in the DTA($p=0.014$), percentage of energy loss in DTA (0.007), PSV in the FL ($p = 0.03$), circumferential WSS in the TL($p=0.022$) and FL($p= 0.047$) showed statistically significant difference between stable size versus enlarging aorta size. Positive association with growth rate was noted with parameters like FLRF ($r=0.71$, $p=0.003$), energy loss in the DTA ($r = 0.56$, $p = 0.007$), percentage of energy loss in DTA($r = 0.62$, $p=0.013$), circumferential WSS in the FL $r = 0.46$, $p = 0.022$ and TL($r = 0.56$, $p = 0.008$). No significant association was noted with parameters like PSV in FL ($r = 0.51$, $p = 0.055$). Multivariate analysis of these parameters showed FLRF($p<0.001$) and energy loss in the DTA ($p= 0.048$) are associated with independent predictors of the progression of the dissection with model adjusted $R^2=0.88$.

Conclusion: 4D flow MRI can help in qualitatively as well as quantitatively assessing patients with type B aortic dissection. False lumen regurgitation fraction and the percentage amount of energy loss in DTA help in predicting the growth of the aneurysm at an early stage in uncomplicated type B dissection helping in the early initiation of treatment in those subsets

1 INTRODUCTION

Aortic dissection (AD) involves intimal or medial tear of the aortic wall with the propagation of tear resulting in the creation of true lumen (TL) and false lumen (FL)(Riambau et al., 2017). It is an uncommon disease with an incidence of about 2.5 - 4.4 per 100 000 person-years and high mortality (DeMartino et al., 2018; Melvinsdottir et al., 2016). Stanford classification which is the most widely for management is based on the location of dissection flap. In Stanford Type B aortic dissection intimal tear is seen distal to the left subclavian artery. The dissection can lead to either thrombosis of the false lumen with expansion of true lumen resulting in favorable prognosis or aneurysmal expansion and rupture of the false lumen leading to high mortality. High flow within the false lumen leads to the persistence of false lumen with aneurysmal expansion. Management depends on the duration and complications at the time of presentation. For acute complicated type B aortic dissection with malperfusion or rupture, management as per the latest ESVS guidelines is emergency thoracic endovascular aortic repair (TEVAR)(class I recommendation)(Riambau et al., 2017).

There is a gray zone regarding the treatment of uncomplicated type B aortic dissection(uTBAD) with no definite treatment guidelines to date.

Recommended treatment includes medical management (by beta blockers and antihypertensive agents) with periodic imaging follow-up (CT angiography or MR angiography) to look at the change in the size of the aorta. TEVAR or open surgical repair is recommended when there is a rapid size of the aorta. Complication rates

remain high in uTBAD, with 25%–30% progressing toward complication within the first 14 days. Long-term outcomes are poor with 30% of medically managed patients experiencing clinically significant aneurysmal degeneration in the first 4 years. Thus there has been increasing interest in the prophylactic management of uTBAD with TEVAR before complication onset. However, TEVAR itself carries risks such as retrograde type A dissection, stroke and paraparesis there is a necessity for appropriate risk stratification in patients with uTBAD. With the high reported number needed to treat (NTT) of 13 with TEVAR to prevent one aorta-related mortality, a substantial opportunity for improved risk stratification and cost-effective care is needed. Therefore, better diagnostic tools are needed that can better discern which patients with uTBAD will eventually experience complications and thus require TEVAR, and which will have satisfactory outcomes with medical management alone.

4D flow MRI is a time-averaged three-dimensional flow imaging(Azarine et al., 2019) that provides information related to flow patterns in the vessel. It can help to estimate the flow dynamics in the true lumen, false lumen, and regurgitation at the entry tear in multiple dissections. These dynamics might predict the persistence of false lumen and thus enable to identify prospectively the rapid growth of the aorta ensuring early treatment in the needed cases. Since few studies address this issue, our study attempts to assess the relation of flow parameters in uncomplicated descending aortic dissection to predict the growth rate.

AIMS AND OBJECTIVES

1. To assess qualitative and quantitative flow parameters in uncomplicated descending aortic(type B) dissection by using 4D flow MRI.
2. To assess the relationship between the change in 4D flow parameters with the expansion of false lumen in type B aortic dissection

Hypothesis- Can 4D flow MRI predict the expansion of false lumen/aorta in the descending aortic dissection cases.

Null hypothesis- There is no difference in the multiple quantitative and qualitative parameters of 4D flow MRI between uncomplicated acute type B aortic dissection which shows significant expansion, and which are stable

Alternate hypothesis: There is a significant difference in the multiple quantitative and qualitative parameters of 4D flow MRI between uncomplicated acute type B aortic dissection which shows significant expansion, and which are stable.

2 LITERATURE REVIEW

Introduction and demographics:

Aortic dissection (AD) involves intimal/medial tear of the aortic wall with the propagation of tear resulting in true lumen (TL) and false lumen (FL)(Riambau et al., 2017). Conditions that cause weakening of the aortic wall or those which increase stress on the aortic wall lead to initiation and propagation of the tear. The incidence of acute aortic dissection ranges from 2.5 - 4.4 per 100 000 person-years in multiple studies (DeMartino et al., 2018; Melvinsdottir et al., 2016). They are more common in men with nearly two-third of involvement had a mean age of 63 years(Evangelista et al., n.d.). Since most patients die before reaching the hospital, the true incidence of acute aortic dissection might be higher. A study by Melvinsdottir et al showed nearly one in five patients with acute aortic dissection expired before reaching hospital(Melvinsdottir et al., 2016). Acute dissections in the ascending aorta have a very high mortality rate reaching 1% per hour(Anagnostopoulos et al., 1972). Even with operative management, mortality is high in ascending aortic dissection with a 30- day mortality of around 17%(Conzelmann et al., 2016). In acute dissections involving descending aorta, in-hospital mortality is about 10% with long-term mortality rate of around 25% at 3 years(Tolenaar et al., 2014; Tsai et al., 2006).

Various classification systems have been proposed to assess the severity of the disease and guide treatment. These are based on the location of the dissection flap since the involvement of ascending aorta has high mortality due to coronary involvement and pericardial tamponade. Stanford classification is the most widely

used and helps in guiding the treatment. It is based on the location of the dissection flap and does not provide information related to the distal extent of dissection.

Stanford Type A AD involves dissection in the ascending aorta regardless of entry tear whereas type B aortic dissection involves dissection distal to the left subclavian artery (LSCA)(Czerny et al., 2019; Riambau et al., 2017). Stanford Type A aortic dissection is seen in nearly 67% of the patients whereas type B is seen in nearly 33% of the patients (Evangelista et al., n.d.). The DeBakey classification which was used previously provides information related to the distal extent of tear in addition to entry tear (as shown in figure 1). The recent SVS/STS reporting standards on aortic dissection have proposed an extensive classification that provides information related to the entry tear and full extent of dissection(Lombardi et al., 2020).

Based on the time at presentation, AD is divided into hyperacute (within 24 hours), acute (2-7 days), subacute(8-30 days), and chronic(>30 days)(Booher et al., 2013). The time of onset is important as high mortality rate was noted in the initial period of the disease as compared to later stages.

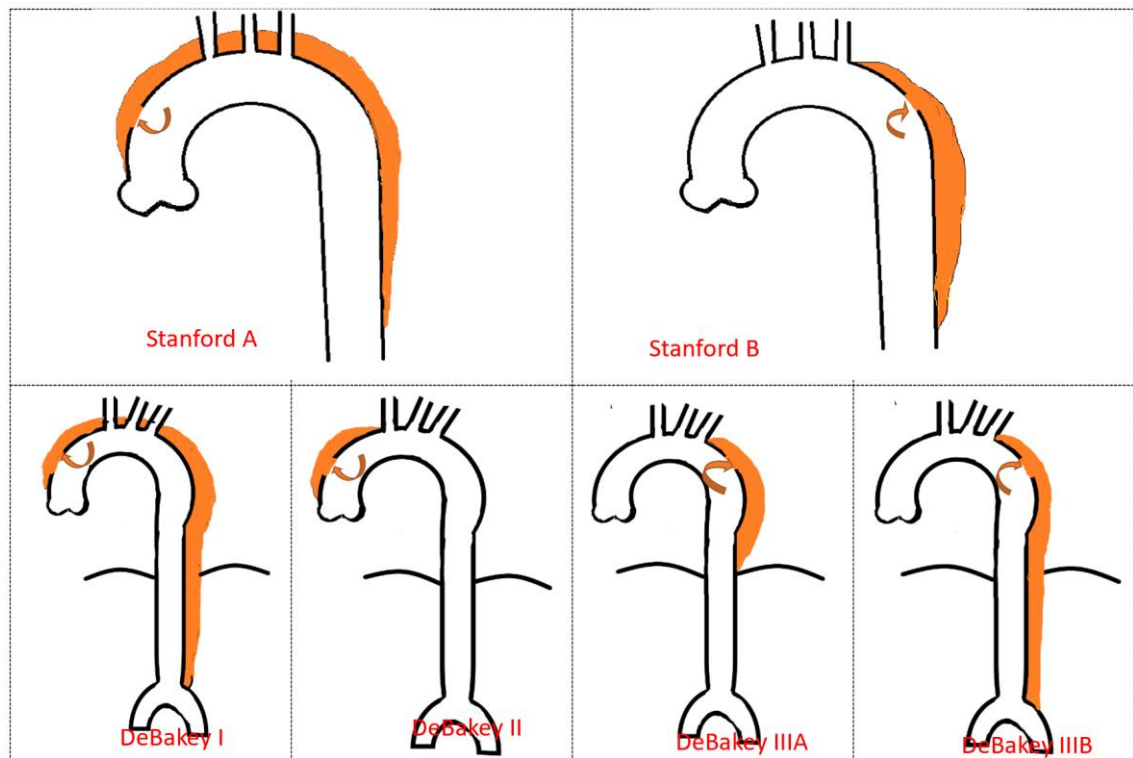


Figure 1 Stanford and DeBakey Classification

Top row shows the Stanford classification, bottom row shows DeBakey classification. Stanford Type A had a dissection flap in the ascending aorta whereas type B has an entry tear distal to the left SCA. In DeBakey, I and II had an entry tear in the ascending aorta similar to Stanford type A. In type I ascending and descending aorta are involved whereas in type II only ascending aorta is involved. In DeBakey IIIA and IIIB involves descending aorta similar to Stanford type B. IIIA involves descending aorta whereas IIIB involves descending and abdominal aorta.

Risk factors:

Conditions leading to the increase in the intimal shear stress or decrease in the arterial wall strength lead to the intimal tear and further progression. The most common risk factor is systemic hypertension which is seen in nearly 80% of the patients and other risk factors include increased age, atherosclerosis, trauma and

iatrogenic cause (Evangelista et al., n.d.). Collagenopathies like Marfans syndrome (MS), Ehlers-Danlos syndrome (EDS) and Loeys-Dietz syndrome (LDS) leads to structural weakness of the intima resulting in dissections (Riambau et al., 2017). Patients with bicuspid aortic valves are also predisposed to aortic dissection at a young age due to inherent aortopathy(Evangelista et al., n.d.).

Clinical presentation:

Clinical presentation is different in type A and type B aortic dissection. The most common presentation seen in these patients is acute onset of excruciating pain in the chest or interscapular region(Riambau et al., 2017). Severe anterior chest pain is more common in type A (79%) than in type B(63%). Interscapular pain is more common with type B (64%) than type A(43%). Patients with type A aortic dissection can present with syncope (seen in nearly 19%) due to severe complications such as cardiac tamponade and dissection extending to cranial vessels resulting in stroke (Evangelista et al., n.d.). Other presentations include acute hypotension due to rupture of the aorta, and visceral or limb malperfusion(Riambau et al., 2017).

Management:

Management of Type A aortic dissection involves immediate surgical management. Management of type B aortic dissection depends on the presentation whether the patient is having complications or high-risk features as described in table 1. The presence of either of these requires immediate treatment whereas uncomplicated cases may be kept under optimal medical management(MacGillivray et al., 2022). As per the 2017 ESVS guidelines, acute complicated type B aortic dissection should be managed immediately (preferably in the subacute phase) by endovascular management by endovascular repair(TEVAR) (Class I

recommendation). Open surgical repair is recommended for those who have unsuitable anatomy for TEVAR (Class IIA) (MacGillivray et al., 2022).

Management of uncomplicated Stanford's type B aortic dissection is debatable. The widely used treatment option is optimal medical management and periodic imaging follow-up (Class I recommendation)(MacGillivray et al., 2022). Optimal medical management includes good control of BP(<120/80 mm Hg) and heart rate(<70 beats/min)(MacGillivray et al., 2022). Beta-blockers are the first-line drugs for medical management. Calcium channel blockers can be considered in those who are intolerant or do not respond to beta blockers. The use of beta blockers in aortic dissection is a class Iia recommendation and calcium channel blockers are the class Iib recommendation as per 2017 ESVS guidelines(Riambau et al., 2017).

Imaging follow-up is by cross-sectional imaging at 1 month, 3 months, 6 months, 12 months, and annually thereafter (Fleischmann et al., 2022; Lombardi et al., 2020). Beyond 5 years of follow-up, the imaging interval can be increased to 18 months or 24 months in case of stable disease. The most used imaging modality is contrast-enhanced CT angiography with an optional plain scan(Fleischmann et al., 2022). MRA is an acceptable alternative to CT angiography due to the lack of radiation. Non-contrast MRA is an alternative technique in patients who are contraindications to gadolinium and iodinated contrast medium(Fleischmann et al., 2022).

Table 1 Complicated, high risk and uncomplicated TBAD

Complicated	High-risk features	Uncomplicated
rupture	refractory pain, refractory HTN	no rupture

malperfusion	bloody pleural effusion,	no malperfusion
	radiographic only malperfusion	no high risk features.
	entry tear along lesser curvature	
	aortic diameter > 40 mm	
	false lumen > 22 mm	

Dynamics of uncomplicated type B aortic dissection- natural history and risks

The inner wall of the false lumen lacks smooth muscle cells and consists predominantly of fibroblasts which proliferate leading to thick, fibrosed non-mobile flap in the chronic phase (Fleischmann et al., 2022). The mobile membrane in acute or subacute stages leads to the decreased pressure difference between true and false lumen whereas the stiff membrane in chronic phases increases pressure in false lumen especially in diastole, resulting in expansion of false lumen as well as overall aorta size (MacGillivray et al., 2022). In addition, the mismatch between inflow and outflow in the false lumen leads to compression of the true lumen in the early phase and aneurysm formation in the chronic phase (Sailer et al., 2017). More blood entry into the false lumen due to large entry tear and poor outflow due to small re-entry tears or no branch vessels leads to increased pressure in the false lumen resulting in enlargement of the aorta (MacGillivray et al., 2022; Sailer et al., 2017).

Keeping the patients on best medical management alone can delay the expansion of the aorta but fails to improve the remodeling of the aorta. Aneurysmal expansion of the aorta was noted in nearly 75% of the patients who were kept on medical management in uncomplicated cases (Fattori et al., 2013). Interventions such

as TEVAR result in the sealing of the entry tear leading to decreased flow in the false lumen. TEVAR is recommended when the size of the aorta reaches more than 55 mm or 60 mm, rapid aortic growth of more than 10 mm/year, or in the symptomatic case(MacGillivray et al., 2022). The benefit of TEVAR in uncomplicated type B cases was shown in the Instead XL trial where patients who were followed up for 5 years showed overall mortality (11.1% vs 19.3%; P=0.13) and aorta-specific mortality (6.9% versus 19.3%; P=0.04) better for TEVAR group compared to optimal medical management (Christoph A, n.d.). Even though TEVAR is associated with complications in the early stages benefits are noted at the 5 years follow-up with a number needed to treat is 13(Christoph A, n.d.).

Timing of TEVAR is also important because TEVAR in the early phase results in the better approximation of the flaps owing to thin flaps whereas thick flaps in the chronic stages lead to suboptimal approximation of flaps thereby persistence of false lumen. TEVAR in the early stage results in positive remodeling of the aorta (MacGillivray et al., 2022). Positive remodeling of aorta is defined as the decrease in size of false lumen, expansion of the true lumen or the reduction in the overall size of the aorta(Lombardi et al., 2020). TEVAR is not without complications. This is a costly procedure and is associated with complications such as type I endoleaks which were seen in 6.9%(Xiang et al., 2021), and retrograde type A AD in 2.5%(Chen et al., 2017). Mortality associated with RTAD was 37.1%(Chen et al., 2017). This is more common in cases of aortic dissection as compared to aneurysms (relative risk was 5.33 (95% CI, 2.70–10.51) and in acute cases as compared to chronic cases(relative risk was 1.81 (95% CI, 1.04–3.14)(Chen et al., 2017). Other complications seen are spinal injury and conversion to

surgery(Christoph A, n.d.). So, pre-emptive TEVAR in all the patients with uncomplicated type B AD is also not advised and subjecting the patients without any risk who might benefit from optimal medical management to dreadful complications from TEVAR(Sailer et al., 2017).

Need for better study in uncomplicated type B dissection(uTBAD) ?

Complication rates remain high in uTBAD, with 25%–30% of uncomplicated cases progressing toward complication within the first 14 days. Long-term outcomes are poor with 30% of medically managed patients experiencing clinically significant aneurysmal degeneration in the first 4 years nearly 40% will eventually require surgical intervention. With a 3-year mortality rate of around 25%, there has been increasing interest in the prophylactic management of uTBAD with TEVAR before complication onset. However, TEVAR itself carries risks such as retrograde type A dissection, a rare but potentially lethal complication with a mortality rate of 37.1%. Other rare devastating procedural complications, such as stroke and paraplegia underscore the necessity for appropriate risk stratification in patients with uTBAD. With the reported number needed to treat with TEVAR to prevent one aorta-related fatality is 13, a substantial opportunity for improved risk stratification and cost-effective care is needed. Therefore, diagnostic tools are needed that can better discern which patients with uTBAD will eventually experience complications and thus require TEVAR, and which will have satisfactory outcomes with medical management alone.

Cross-sectional imaging like CT angiogram and MR angiogram provides information related to the morphology of the dissection with less information related

to the flow. Literature related to CT angiography in predicting future adverse events is less. In one study by Sailer et al in 83 patients, showed CT parameters like the circumferential extent of FL in degrees, maximum aortic diameter, outflow from FL, and the number of intercostal arteries allowed stratification of patients at 2 years into low, intermediate, and high-risk groups with a risk of 7.4%, 20.6%, and 54.4% respectively(Sailer et al., 2017). Other parameters like size of the ET and location of ET showed poor risk prediction(Sailer et al., 2017). The other anatomical parameters which have been studied for risk assessment are given in table 2.

Table 2 Morphological high-risk features which can result in rapid aortic growth

High-risk feature (reference)	Cause of expansion of dissection
False lumen circumferential extent >249 degrees (Sailer et al., 2017)	Greater circumferential extent had more aortic tissue of the thin FL wall, so more chance to dilate
Primary ET within 5 cm of LSCA (Tolenaar, van Keulen, Trimarchi, et al., 2013)	FL is subjected to higher forces.
Elliptical configuration of TL vs circular(Tolenaar, van Keulen, Jonker, et al., 2013)	Elliptical shape is due to high pressure in false lumen compressing the TL
Single entry tear vs multiple ET(Tolenaar, van Keulen, Jonker, et al., 2013)	Single large tear increases pressure in the FL whereas multiple tears lead to depressurisation of FL due to more outflow

4D flow MRI

4D flow is a novel technique that provides flow-related information in all three directions. As the flow information is directly related to the serial change in the aortic diameters it might help in better predicting patients who can have rapid aortic growth.

Physics and parameters of 4D flow

Velocity information in the MRI can be achieved with either 2D phase contrast or 4D flow. In the 2D phase contrast, images are obtained with single direction VENC during breath hold. The plane should be exactly perpendicular to the flow in the vessel to obtain correct velocity information. Acquisition in case of complex diseases like aortic dissection is difficult and requires scans to be repeated multiple times in multiple planes. 4D flow MRI is a time-resolved, three-dimensional phase contrast MRI sequence that provides 3D volume information over a period(Azarine et al., 2019). It has three velocity images in 3 directions and one magnitude image. A large volume of the aorta can be acquired in a single acquisition followed by the retrospective analysis of various parameters by drawing the region of interest at the required site(Burris et al., 2019). The advantage of 4D flow over 2D phase contrast acquisition is that the plane of velocity assessment can be retrospectively selected in the post-processing software in the 4D flow (Azarine et al., 2019).

Sequence acquisition and parameters:

For the flow information to be achieved, it needs to be synchronized to ECG gating. Retrospective gating enables coverage of the entire cardiac cycle compared to prospective gating. Respiratory motion affects the 4D flow data and it takes about 8-10 minutes for the sequence to complete thus requiring respiratory gating techniques (respiratory navigator echo, PACE). The usual Sequence used for 4D flow is a spoiled gradient sequence with short TE and TR (TE= 2-4 msec, TR= 5-7 msec).

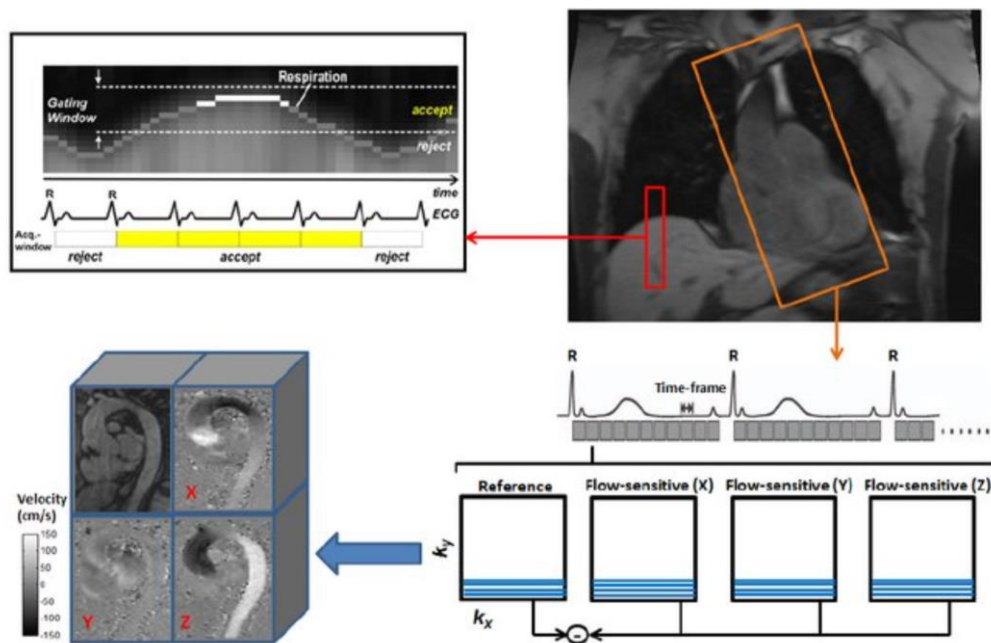


Figure 2 basic acquisition of 4D flow

With the ECG and respiratory navigator acquisition, 4D flow sequence is acquired. It included one magnitude image and 3 phase images in 3 directions.

Analysis of the 4D flow:

It involves qualitative and quantitative analysis. The qualitative analysis includes gross visualization of the flow, velocity vectors, streamlines, and path lines.

Qualitative analysis:

- Color-coded velocity images: They provide information related to the gross visualization of the direction of flow and velocity of the flow.
- Velocity vectors: provide information related to the speed and direction of the flow. The arrow of the vector points to the direction of flow, the color of the vector determines magnitude of flow.
- Streamlines determine the path a particle takes when it is released into the velocity field. Normal flow in the arteries is laminar. Streamlines show helical or vortical flow in aortic dissection due to acceleration of blood flow at the site of entry tear causing turbulence in the blood flow which results in spiral folding of the blood flow creating vortices. This results in high-velocity jet imping focally on the wall(Saitta et al., 2021). In vortical flow, blood will be recirculation from the main flow direction resulting in the swirling motion as in whirlpools. Vortical flow is graded as follows. Grade 0- laminar flow with no helices or vortices. Grade 1- mild helical or vortical flow (< 360 degrees of rotation), Grade 2- severe helical or vortical flow(>= 360 degrees of rotation)(Takahashi et al., 2021)
- Path lines show blood flow in the 3-dimensional plane over one or more heartbeats. Normal flow in the arteries is laminar with high velocity noted in the center of the lumen as compared to the periphery(Azarine et al., 2019).

Quantitative analysis:

They include

- Basic quantitative parameters: After segmentation of the part where the flow information is to be studied an ROI is to be drawn at the vessel of interest. The software automatically propagates the ROI in all the cardiac frames; however, it is ideal to check all the frames to avoid measurement errors from the inclusion of nearby field. Various flow information currently available with the software are forward flow(ml/beat), peak systolic velocity of that vessel(centimeters/second), reverse flow(ml/beat), and regurgitation fraction(percentage)(Azarine et al., 2019).
- Wall shear stress- Wall shear stress is the shear force that is exerted tangentially on the vessel wall by the moving viscous blood(Ferdian et al., 2021). Wall shear stress is decomposed into axial (through plane) and circumferential (in-plane) wall shear stress. WSS parameters derived from 4D flow are maximum WSS, average WSS, average axial WSS, average circumferential WSS. In cases of laminar flow, there will be increased axial WSS whereas in case of helical flow there will be circumferential WSS(Rodríguez-Palomares et al., 2018).
- Energy loss across lumen:
- Turbulent kinetic energy: it is the energy stored in the turbulent flow and this is dissipated as heat. Blood flow turbulence is expressed as rapid velocity fluctuations within a single imaging voxel(Catapano et al., 2020).

- Viscous energy loss: it is the non-turbulent mechanical energy converted irreversibly into heat. It is measured per volume units. Here viscous dissipation is calculated using reformulation of the viscous portion of the incompressible Navier-Stokes energy equation(Barker et al., 2014; Catapano et al., 2020). Here energy loss due to complex flow can be accounted as well as regions of permanent energy loss are visualized(Barker et al., 2014).
- Pressure loss across lumen: It is relative pressure measurements that can be achieved with the 4D flow(Marlevi et al., 2021). Color maps show distribution of pressure in the vessel during the cardiac cycle(Catapano et al., 2020).

Evidence for 4D flow in Type B dissection – the current scenario

Takahashi et al showed that high amount of FL flow and velocity leads to higher vortex grade in 32 patients having aortic dissection using multi VENC 4D flow MRI. Patients with more complication showed higher vortex grade [2 (IQR 1–2) vs 0 (IQR 0–2); P = 0.01] in comparison with stable disease(Takahashi et al., 2021). Higher vortical flow resulted in more rate of complication when compared to the patients with stable disease(Takahashi et al., 2021).

False lumen ejection fraction:

Increased pressure in the false lumen shows decreased velocity at the site of the dominant entry tear and there will be increased retrograde flow through the false lumen as the outflow is poor(Burris et al., 2019). This was shown in a prospective study by Burris et al in 18 patients where increased false lumen ejection fraction

(ratio of retrograde flow during diastole with the antegrade flow during systole) lead to increased aortic growth in comparison with cases having stable disease(Burris et al., 2019). A similar observation was noted in another prospective study in 12 patients by Marlevi et al that increased retrograde flow across false lumen resulted in the growth of the false lumen(Marlevi et al., 2021).

Relative pressure change:

Direct measurement of the pressure is possible with catheter angiography, but it has its own complications and is seldomly done for the routine diagnostic purpose(Burris et al., 2019). In 4D flow relative pressure measurements can be taken. In the study by Marlevi et al, showed an increase in relative pressure changes across false lumen resulted in the growth of the false lumen, thereby helping in predicting potential candidates for early intervention(Marlevi et al., 2021).

Energy loss:

High energy loss in a particular segment results in energy dissipation from the flowing blood into the adjacent aorta wall leading to the rapid degeneration of the aortic wall at that segment(Qiao et al., 2022). Sudden expansion of the aorta leads to turbulent flow at the borders resulting in increased energy loss. The more the turbulent kinetic energy the harder heart need to work(Sträter et al., 2018). Greater fluctuations of blood flow in turbulent areas require more energy to maintain blood flow(Sträter et al., 2018). There are four sources of energy loss noted in the aorta. These include viscous friction, turbulence dissipation, wall deformation, and local lesions. Viscous friction of the blood leads to the excess amount of energy loss followed by the aorta deformation. Excess energy loss in a particular segment of

aorta leads to rapid deterioration of that segment. In the normal aorta, branch points are the areas where there was the high amount of time-averaged viscous dissipation, so these areas are more prone to lesions(Qiao et al., 2022).

Wall shear stress:

. Abnormal wall shear stress is one of the key determinants in the initiation of dissection(Pirola et al., 2019). High WSS leads to the initiation of dissection as well as degeneration of the extracellular matrix and elastic fibers. Low shear stress leads to thrombus formation of the false lumen(Pirola et al., 2019). In a study using 4D flow MRI in 54 patients by Ruiz-Muñoz et al showed that in-plane rotational flow and percentage of thrombus in the false lumen correlated positively with aortic growth ($p= 0.006$, and 0.037 , respectively)(Ruiz-Muñoz et al., 2022). Wall shear stress showed a trend for a positive association ($p = 0.060$) in predicting aortic growth(Ruiz-Muñoz et al., 2022). Rotational flow results in more stress on the aortic wall leading to increased aortic growth(Ruiz-Muñoz et al., 2022).

Table 3 Studies related to 4D flow MRI in aortic dissection was summarized in the following table

Author	Parameter studied	Study characteristics	Key Results
Shang et al(Shang et al., 2015)	Percentage of false lumen flow TAWSS	CFD in 14 ATBAD 7- rapidly expanding, 7- stable disease	Rapid aortic growth had high flow through false lumen. (78.3% ± 9.3% vs 56.3% ± 11.8%; $P = .016$) WSS on aortic wall was higher (12.6 ± 3.7 vs 7.4 ± 2.8 Pa; $P = .028$)
Liu et al (Liu et al., 2018)	TL, FL flow and velocity	16 patients	Large initial ET size correlated positively with average velocity, average net flow, and peak flow in the false lumen($p<0.05$), peak flow was reduced in FL with increased intimal tears($p=0.025$)
Takahashi et al(Takahashi et al., 2021)	FL flow and velocity Vortical flow	32 patients multi VENC 4D flow MRI	Patients with more complication showed higher FL flow [41.7 (interquartile range, IQR 29.1–59.7) vs 17.7 (IQR 9.0–42.0) ml/s; $P = 0.01$], higher vortex grade [2 (IQR 1–2) vs 0 (IQR 0–2); $P = 0.01$]
Burris et al(Burris et al., 2019)	FL Ejection fraction	18 patients	Increased false lumen ejection lead to increased aortic growth in comparison with cases having stable disease
Marlevi et al(Marlevi et al., 2021)	FL retrograde flow relative pressure across FL	12 patients	Increased retrograde flow across false resulted in the growth of the false lumen Increase in relative pressure changes across false lumen resulted in growth of the false lumen
Ruiz Muñoz et al(Ruiz-	in plane rotational flow	54 patients	In plane rotational flow correlated positively with aortic growth ($p= 0.006$)

Muñoz et al., 2022)	WSS		WSS showed a trend for a positive association (p = 0.060) in predicting aortic growth
Jarvis et al.(Jarvis et al., 2020)	TL, FL Turbulent kinetic energy	20- descending aortic dissection 21- controls	repaired TAAD had high TL kinetic energy, FL kinetic energy and FL statis as compared to TBAD as well as controls

Summary of review of literature with lacunas in literature

CT angiography and MR angiography provide information related to the morphological parameters of the dissection including size of true lumen, false lumen and entry tear size. Treatment is also based on these anatomical parameters keeping the patient on anti-impulse therapy till the threshold size is reached. However, these anatomical parameters are not able to predict which patient can have the rapid aortic growth in uncomplicated type B dissection. Some of the patients having small aortic sizes can rapidly progress in a short period, keeping these patients at high risk of rupture and mortality. Imaging of the flow dynamics like velocities in true and false lumens, and stress exerted on the walls of the aorta by turbulent blood are not extensively studied to provide data on the rate of the expansion rate of the aorta. In addition, many of the studies are retrospective where the 4D flow was obtained in the chronic phase which finds only association but not causality. The present prospective study aimed to fill these lacunae to derive 4D parameters which can predict the long-term expansion of the aorta in the acute phase itself in cases of uncomplicated type B aortic dissection so that timely intervention can be done in those subsets who have a high risk for future rupture

3 MATERIALS AND METHODS

Study type:

This is a single-center prospective, observational study done from June 2020 to June 2022 in patients presenting with uncomplicated type B aortic dissection to radiology / vascular surgery OPD. The study was performed after obtaining institutional ethics committee approval (IEC No: SCT/IEC/1617). Informed consent was obtained from all the patients

Inclusion criteria:

Patients detected with uncomplicated acute and subacute Stanford's type B aortic dissection

Exclusion criteria:

1. Patients with multiple lumen type B dissections
2. Patients who are having dissection flaps in the abdominal aorta only without thoracic aorta involvement.
3. Acute complicated aortic dissection.
4. Contraindications to MRI or incomplete CMR examination.
5. Complete false lumen thrombosis in the initial examination
6. Claustrophobic.
7. Those who failed to give consent.

Study design:

This study was performed on consecutive cases presented to our institution with uncomplicated descending type B aortic dissection. All the patients with suspected aortic dissection underwent CT angiography of the thorax to detect the type of aortic dissection. Patients with type B dissections with no signs of complications (such as rupture, malperfusion, and high-risk features like refractory pain, refractory HTN, bloody pleural effusion, radiographic only malperfusion) were included in the study. All these patients underwent 4D flow MRI as an additional sequence within 1 month. The quantitative and qualitative parameters were obtained from 4D flow MRI. The patients were followed up by CT angiography at 1- 2 years after the MRI. The rate of progression is considered as significant when the aortic growth rate at the maximum size is more than 3 mm/ year.

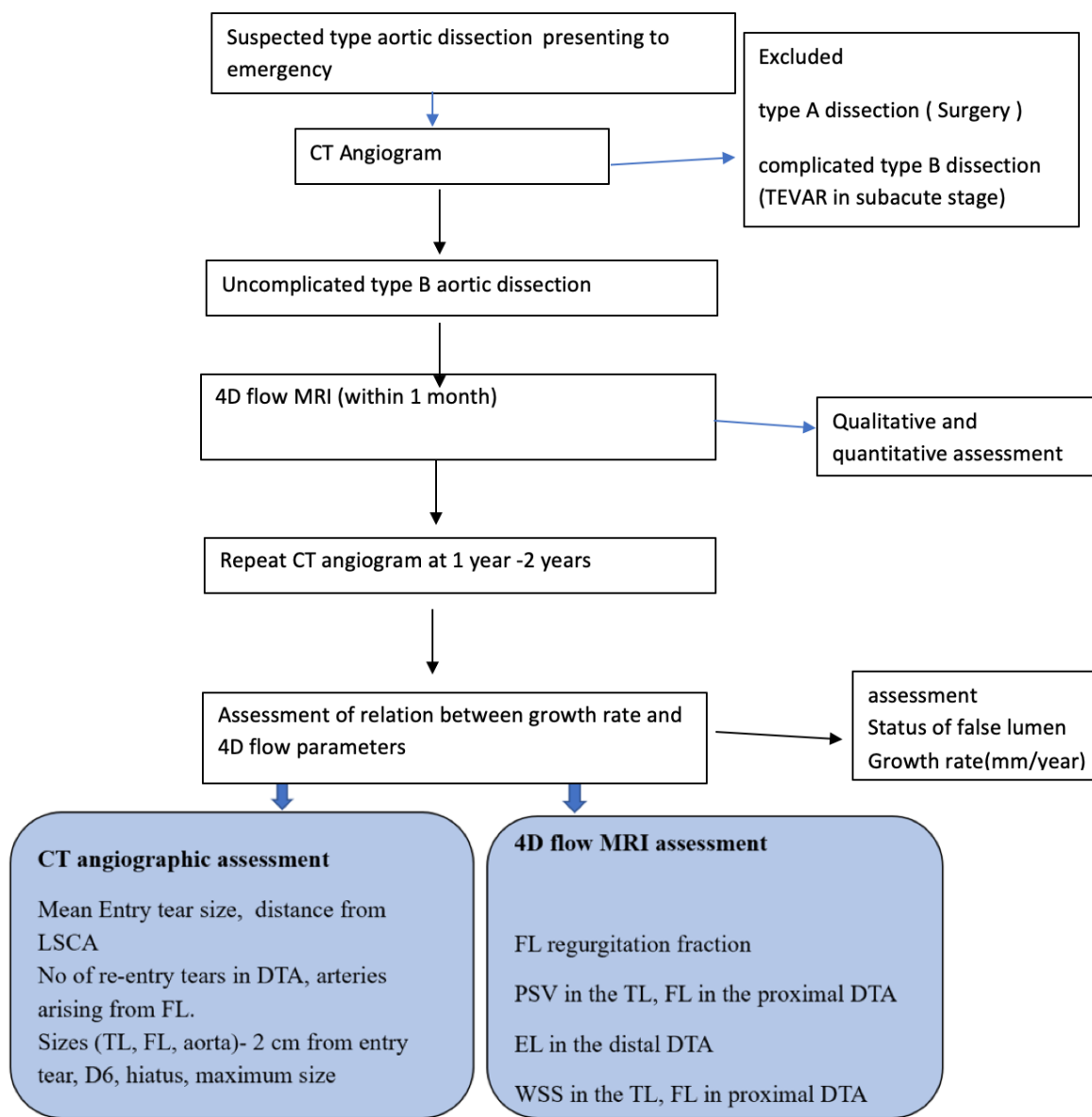


Figure 3 Flow chart showing flow design

The clinical parameters which were obtained at the time of MRI were the age of the patient, gender, hypertension and whether the hypertension was controlled by medication during the follow-up time, pulse rate of the patient, diabetes mellitus, smoking, connective tissue disease, chronic kidney disease.

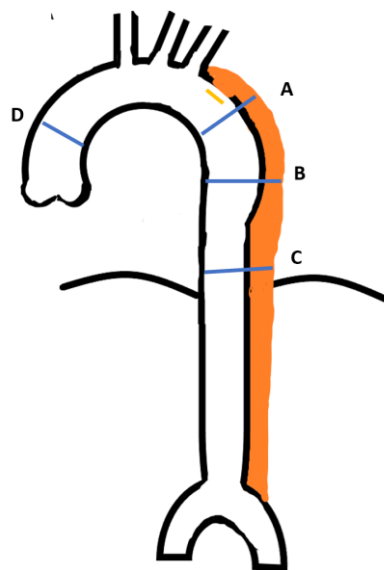
CT angiography protocol:

CT angiography was performed in 256 slices Philips Brilliant CT scanner after injecting iodinated contrast agent (1.5-2 ml/ kg weight) at a rate of 5-6 ml/sec through the right antecubital vein. Contrast agent commonly used was Ominipaque (iohexol) with iodine concentration of 350 mg/ml. Scanning parameters included kVP of 120 millivolts with mAs 210 milliamperes. A non-ECG gating CT angiography was performed from the level of the thoracic inlet up to the level of femoral arteries, followed by the delayed scan of the thoracic segment to look for false lumen thrombosis. Bolus triggering was performed in all the cases by keeping the region of interest at the level of descending aorta. The scan was initiated when the contrast threshold reached 110 HU. Delayed phase was performed 60-70 seconds after contrast injection.

Lesion assessment:

Measurements of the true lumen, false lumen and aortic sizes were measured as per the SVS/STS reporting standards for type B aortic dissection(Lombardi et al., 2020) as shown in figure 5. Measurements were performed in the true axial plane (double axial plane) of the aorta. Sizes were measured are ascending aorta from outer to outer wall. True lumen, false lumen, aorta within 2 cm from entry tear, D6, distal DTA as shown in figure 4. Size of the entry tear in oblique sagittal view, the distance of entry tear from left SCA, number of reentry tears within DTA segments as well as arteries that are arising from false lumen are assessed. False lumen status was observed as it is fully patent, partially thrombosed, or completely thrombosed. It is considered as fully patent when contrast opacification of the FL was noted

completely either in arterial phase (AP) or in delayed phase (DP). In the partly thrombosed false lumen, residual contrast opacification was noted either in AP or DP. In the completely thrombosed FL, no contrast opacification was noted in both the phases. The follow-up CT angiography was also performed with the same parameters. The expansion in CT was measured at the maximum diameter level in both scans. The growth rate was considered as enlarging aorta size or significant if it is more than 3 mm in one year(Sueyoshi et al., 2004). All the CT angiographic measurements were assessed by two cardiovascular radiologists (A.P) and (J.V) who had 3 years and 5 years' experience respectively in cardiovascular imaging



Various measurements taken in the CT angiography are as follows:

- Entry tear size (yellow line)
- Distance from LSCA (blue star)
- TL, FL, aorta size within 2 cm from LSCA(A), D6(B), Hiatus(C), ascending aorta(D)
- Status of false lumen- patent/ thrombosed.
- Number of re-entry tears in DTA.
- Major arteries arising from FL.

Figure 4 Anatomical measurements from CT angiography

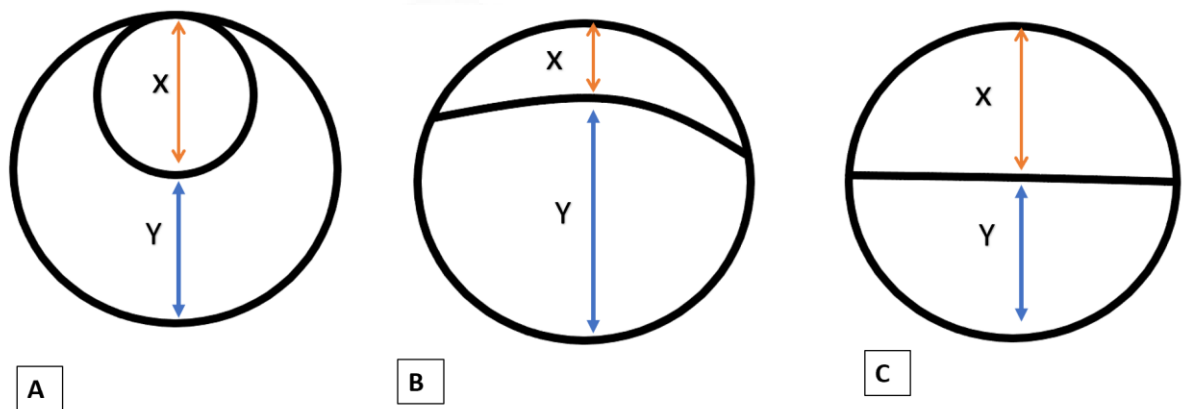


Figure 5 SVS/STS standards for measurement of TL, FL, Aorta sizes in AD:

Showing measurement of TL, FL and Aorta size in varying shapes of dissection flap as per SVS/STS reporting standards for type B aortic dissections. Measurements were performed perpendicular to the dissection flap in the true axial plane. X gives the measurement of TL, Y gives measurement of FL, and X+Y gives total aortic measurements.

4D flow MRI acquisition protocol:

All CMR were performed on 1.5T MRI system (Siemens Avanto fit Version- syngo MR E 11, Germany) using a dedicated 18-channel body matrix coil. After planning the localizer of thorax, scanning was performed in the axial plane from thoracic inlet up to the diaphragm in the free-breathing mode using retrospective ECG gating and respiratory navigator gating. Contrast was not injected in any of these patients.

Scanning parameters included: Slice thickness- 2.5-3 mm, spatial resolution-2.5 mm, temporal resolution- 40 milliseconds, Time to echo(TE)-2.3 milliseconds, Time to

repetition(TR)-38 milliseconds, flip angle-9 degree, matrix size-2.4x2.4x2.5 mm, single VENC of 150 cm/s. Scanning time ranged from 8-10 minutes based on coverage. Patient blood pressure was measured by the brachial cuff, immediately before commencing scanning, while lying on the scanner table outside of the bore.

4D flow MRI processing:

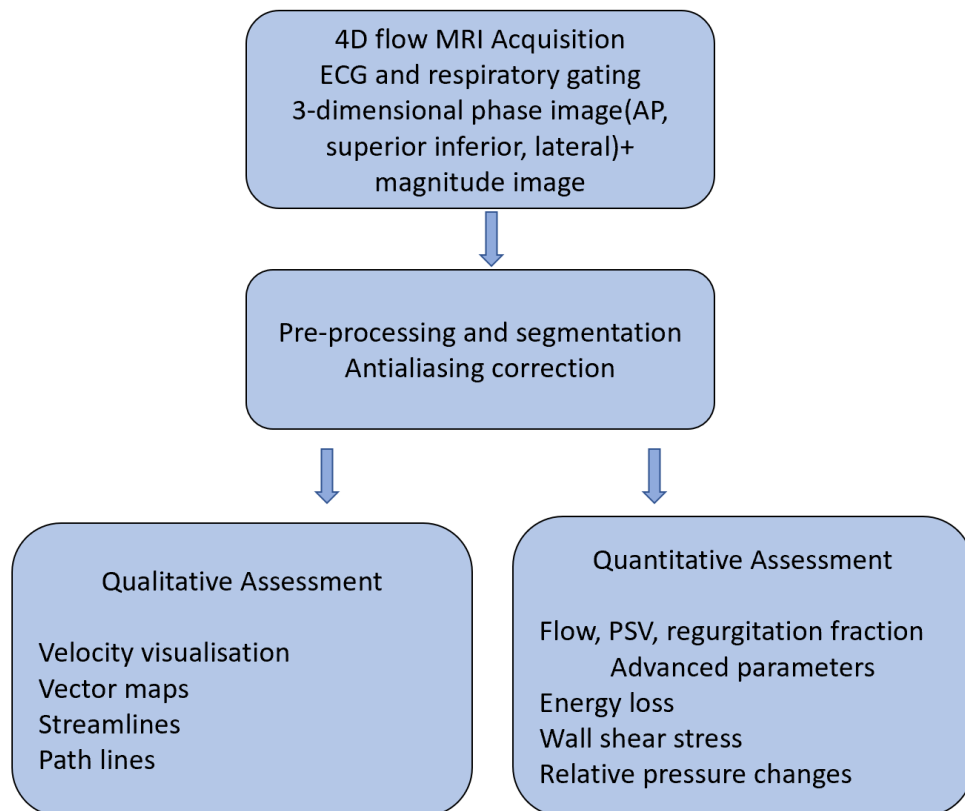


Figure 6 Flow chart showing basic steps in the 4D flow

All the images were processed using Circle CVI 42 software. Offset and anti-aliasing correction was applied before further procession. Anti-aliasing correction reduces aliasing artifacts up to 2 times the VENC. The Center line was drawn from the level of ascending aorta up to the diaphragm and then aorta was segmented from

the rest of the acquisition. True lumen and false lumen are not segmented separately as shown in figure 7. Further assessment was performed in the segmented aorta and the following parameters are assessed. Visual assessment of streamlines and path lines at the site of entry tear and proximal false lumen to look for laminar flow, helical or vortical flow. Vortical flow is graded as 0, 1, and 2 based on the degree of vortices as mentioned earlier.

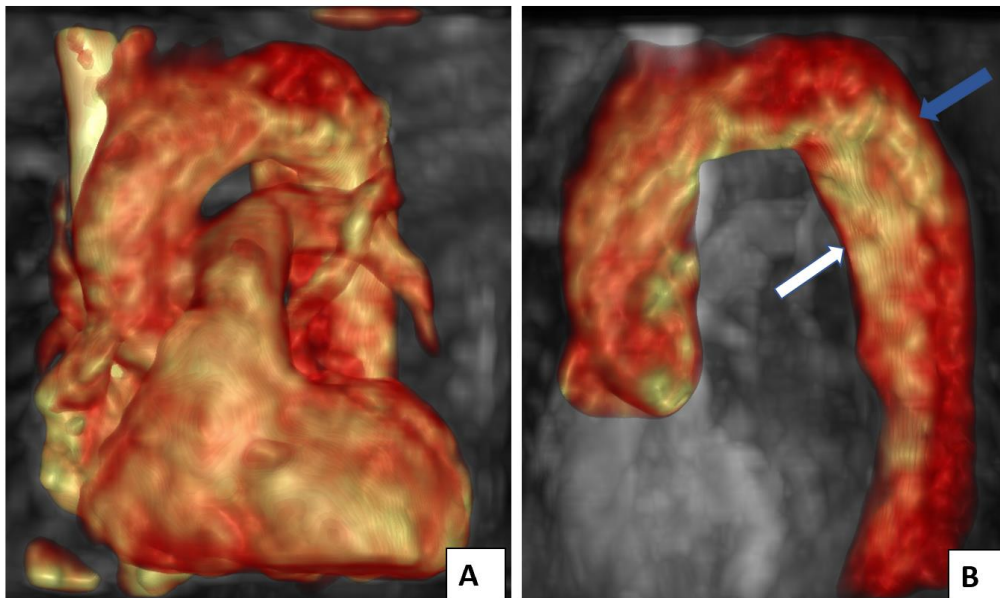


Figure 7 Image showing initial processing step and segmentation of aorta:

Image (A) is showing initial processing which contains phase information related to entire acquisition. Image (B) involves segmentation of aorta by using the center line method and further analysis was performed in the segmented aorta. In this case of aortic dissection, the true lumen (white arrow) and false lumen (blue arrow) are segmented together.

Quantitative parameters assessed are

A . False lumen regurgitation fraction within the first 2 cm of entry tear, PSV in the false lumen and true lumen at this level. This can be acquired by aligning the images in double oblique MPR planes and by drawing the region of interest in the false lumen and true lumen as explained in figure 8.

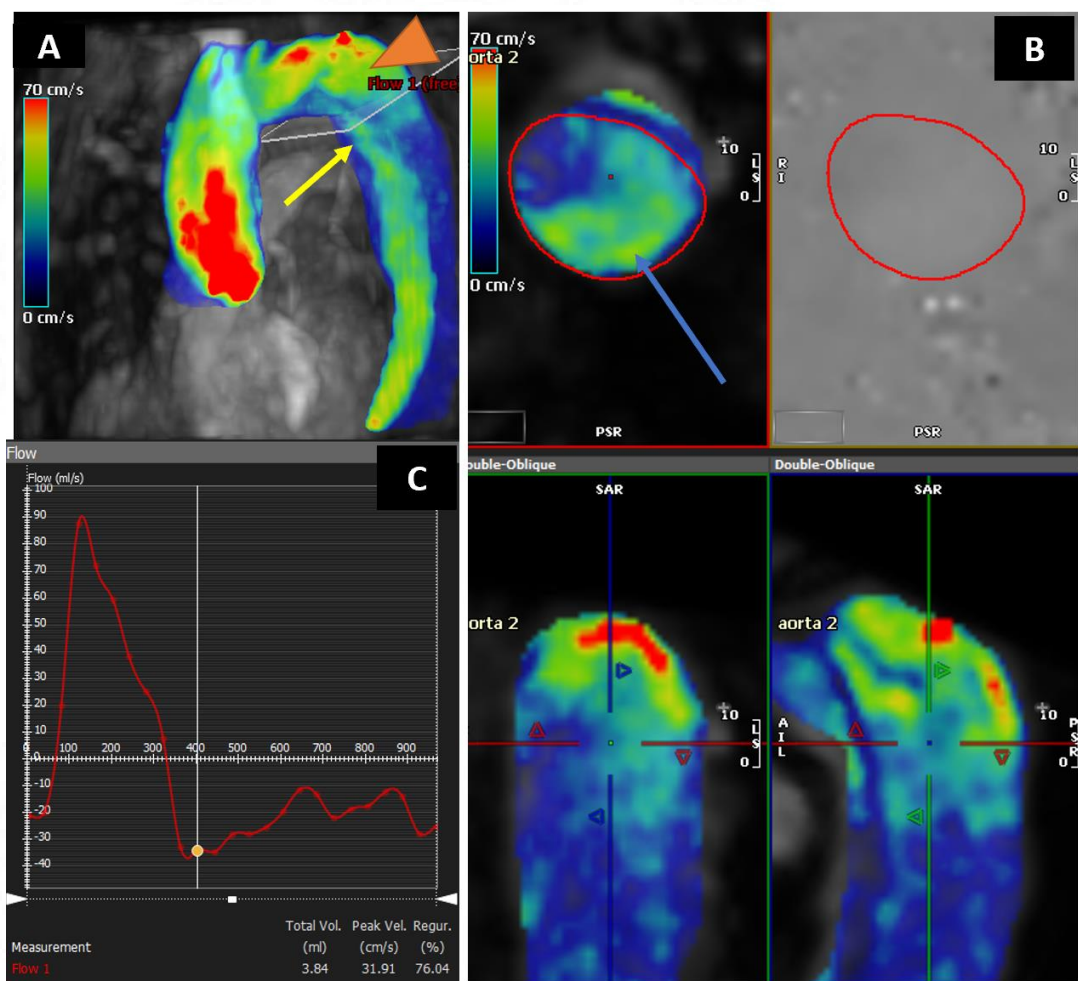


Figure 8 Image showing technique of measuring flow volumes and velocities across vessel lumen

Image (A) is the velocity magnitude image which clearly shows TL (arrow) and FL (arrowhead) and velocity aliasing at the entry tear distal to LSCA. Image (B): In

MPR after aligning cursers in the double axial plane, ROI is to be drawn in the axial images and software automatically propagates ROI through various cardiac frames. Finally flow maps are displaced proving information related to flow(ml/beat), peak systolic velocity(cm/s), regurgitation fraction (%).

B. **Energy loss:** In the present study, viscous energy loss was calculated between two ROIs placed across the segment of the aorta. Software automatically provides viscous energy loss in between two ROI. Initially, EL was calculated from the proximal ascending aorta to the distal DTA, then EL was calculated in the DTA from ET up to distal DTA. The percentage of EL in the DTA to the whole aorta was calculated using the formula.

$$\text{Percentage of energy loss in DTA} = \frac{\text{energy loss in the DTA from the entry tear to distal DTA}}{\text{total energy loss from ascending aorta to distal DTA}}$$

C. **Wall shear stress** was calculated at the level of ascending aorta, true lumen, and false lumen at the maximum size. Wall shear stress components assessed at the ascending aorta are maximum WSS whereas in the true lumen and false lumen average axial and average circumferential wall shear stress were assessed. All the 4D flow MRI parameters were assessed by two cardiovascular radiologists who had 3 years and 5 years' experience in cardiovascular imaging

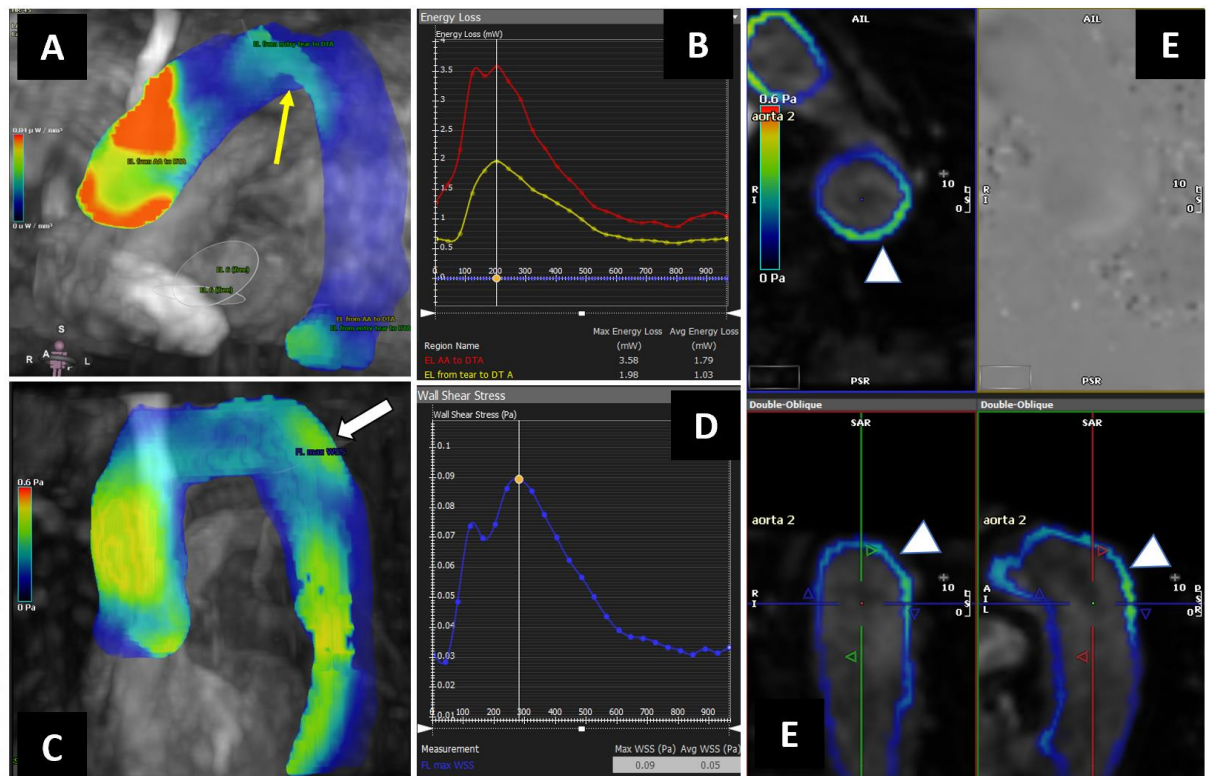


Figure 9 Technique for calculation of energy loss and WSS

Image (A), (B) shows energy loss, (C), (D), and (E) shows WSS images in case of type B AD. In the Magnitude image, there will be two ROI that need to be placed at the ROI of the vessel and the energy loss in microwatts/mm³ was calculated. In image (A) in addition to the energy loss in ascending aorta, there was energy loss in the proximal DTA at the entry tear site (arrow). Energy loss values will be displayed as in image (B). Image (C): WSS magnitude image during systole showing the distribution of WSS across various aortic segments. There was a focal increase in the WSS in the proximal DTA (arrow). Image (D): WSS values. In image E there was a focal increase in the WSS in the outer wall of aorta (arrow heads).

Analysis of results:

The collected data were analyzed with IBM SPSS Statistics for Windows, Version 23.0. (Armonk, NY: IBM Corp). To describe the data descriptive statistics frequency analysis, percentage analysis was used for categorical variables and the mean & S.D were used for continuous variables. Normality was assessed using the Shapiro–Wilk test. Comparison of group means for continuous variables was performed with unpaired t-tests or Mann–Whitney U test. Chi-square analysis and Fisher’s exact test were used to evaluate differences in the frequency of categorical variables. To assess the relationship between the variables Spearman's rank correlation was used. To find the significance in categorical data Chi-Square test was used. Similarly, if the expected cell frequency is less than 5 in 2×2 tables then Fisher's Exact was used. To find the agreement between the observers Bland- Altman plot was used. Pairwise correlation matrices were used to identify multicollinearity amongst predictors. Subsequently, multiple linear regression models with robust standard errors were used to examine the association of hemodynamic metrics with aortic growth after adjusting for baseline aortic diameter. A p-value of < 0.05 was considered significant for all statistical tests.

4 RESULTS

During the time of June 2020 to June 2022, a total of 63 patients with suspected acute and subacute dissection underwent CT angiography. Among them, 32 had type A aortic dissection and 12 patients had complicated type B aortic dissection. So, these patients were excluded. Finally, 19 patients with uncomplicated descending aortic dissection underwent 4D flow MRI within 1 month of the initial CT angiography scan. Among them, 3 patients were excluded due to the poor quality of the imaging. One patient was excluded due to loss of follow-up. Remaining 15 patients underwent CT angiography within 2 years period to calculate the growth rate. Cases having growth rate of more than 3 mm in one year are considered as significant. Various morphological parameters from CT angiogram and flow parameters from 4D flow MRI were assessed. Eight age and sex-matched controls were also taken to validate the sequence and for comparing parameters.

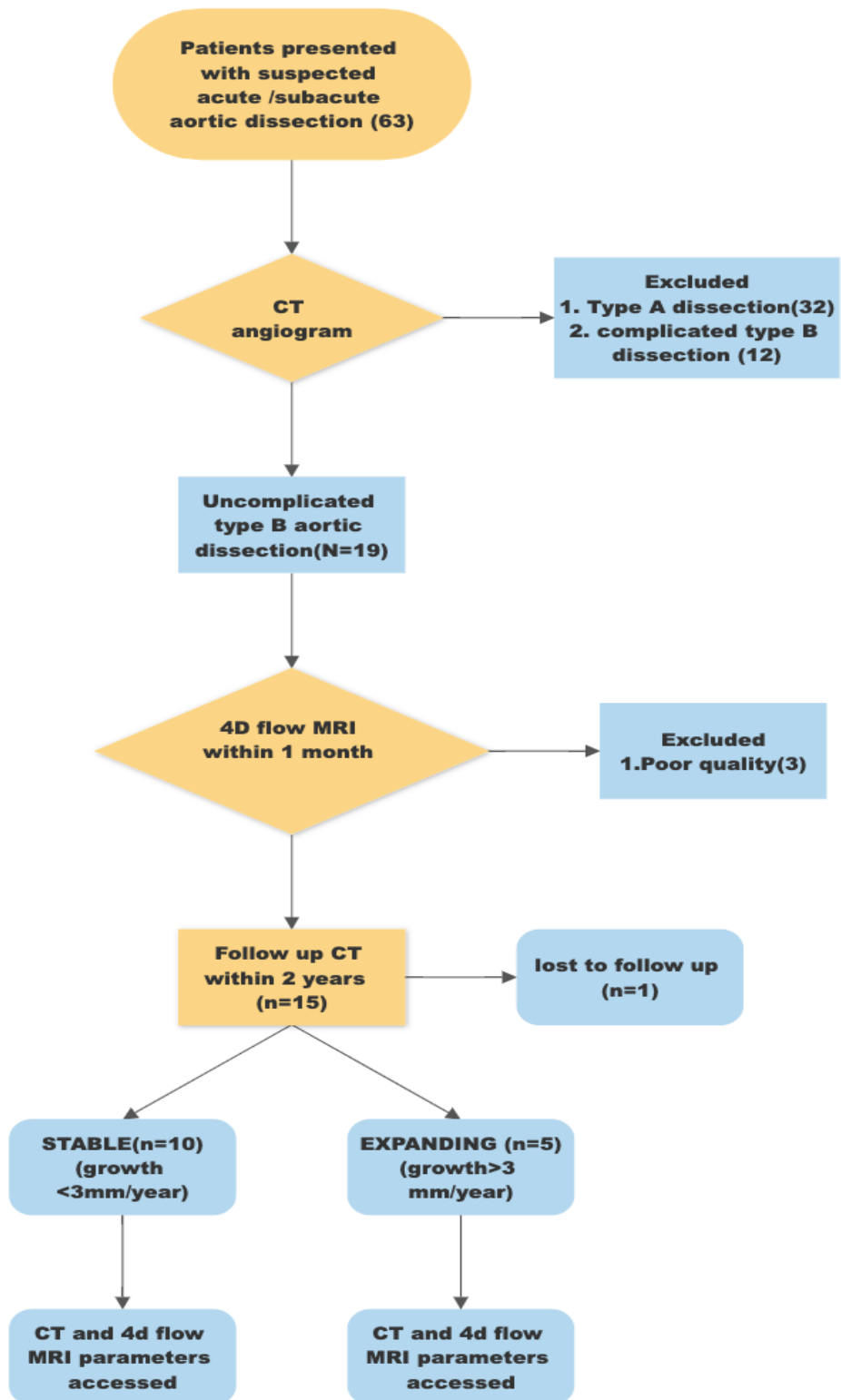


Figure 10 Flow chart of the results

1. Patient characteristics and demographics

12(80%) of the patients were males and 3 (20%) were female. The average patient age was 55.5+/- 8.1 years (ranging 40 -73 years). Hypertension was present in 13/15 (87%) patients. 20% had uncontrolled hypertension despite 3 antihypertensive drugs. Other co-morbidities included diabetes mellitus (13%), smoking (26%), connective tissue disorders (13%), and chronic kidney disease (13%). The age of presentation was less in the patients with the connective tissue disorder (mean age of 47 years as compared to 55 years in the general population). Pulse rate at the time of presentation (b- blockers) ranged from 48- 80 beats per minute with 87% had pulse rate of less than 70 beats per minute. All the patients were on beta-blockers and 8 patients were on ACE inhibitors. 12/15 patients presented in the acute phase (<2 weeks) while 3/15 were in subacute phase (2 weeks-6 weeks)

Table 4 Showing demographic details

Demographics(n=15)	
Age (mean)	55.5+/- 8.1 (40-73)
Sex	Males- 12(80%), females-3(20%)
Hypertension, n(%)	10(83%)
DM n(%)	2(13%)
Smoking n(%)	4(26%)
Connective tissue disease n(%)	2(13%)
Chronic kidney disease n(%)	2(13%)

Uncontrolled HTN n(%)	3(20%)
Pulse rate	(48-80 bpm)
Pulse rate ≤ 70	13(87%) (48-80 bpm)
Systolic blood pressure (at initial presentation after beta blockers)	114.8 \pm 20.4 mmHg
Diastolic blood pressure (at initial presentation after beta blockers)	67 \pm 10 mmHg
Type of presentation	Acute (12/15), subacute (3/15)

2. Anatomical assessment of dissection: In initial imaging

2.1 General anatomic detail in the initial scan

The average maximum aortic diameter was 42.3 \pm 8.2 mm ranging from 30 mm to 58 mm.

Table 5 Anatomic detail in the initial scan

Anatomic parameter	Mean(range)
Maximum diameter aorta at baseline(mean)	42.3 \pm 8.2 mm (30 mm- 58 mm)
Ascending aorta size	34.4 \pm 4.0 mm (26-20 mm)
Aorta size near LSCA	41 \pm 8.8 mm (29-58 mm)
Aorta size at D6 vertebral artery level	34.8 \pm 4.6 mm (24-42 mm)
Aorta size at hiatus	32 \pm 6.1 mm (21-43 mm)

2.2Entry tear characteristics

Eight patients (58%) were having large entry tears (more than 10 mm) with the median size of the entry tear is 11.0 mm ranging from 5 mm to 27 mm. All the patients had the entry tear within proximal DTA. The initial entry tear was at an average of 16.9 ± 15.2 mm from the left subclavian artery (LSCA) (range 2 mm to 41 mm). 13/15 (87%) had an entry tear on the outer surface of the aortic arch. 9/15(60%) of cases had no reentry tears in the DTA, 1(6%) had 1 reentry tear, and 5 (33%) had 2 reentry tears in DTA.

Table 6 Entry tear characteristics

Entry tear characteristics	
Size of entry tear (median)	11.0 \pm 6.3 mm (5-27)
No of the cases having ET>10 mm	8(53%)
Distance of entry tear from left subclavian artery	16.9 \pm 15.2 mm (2mm-41 mm)
Tear in outer wall of aorta	13(87%)
Number of additional tears in DTA	0 tears- 9(60%) 1 tear – 1(6%) 2 tears – 5(33%)

2.3 False lumen(FL) and true lumen(TL)characteristics

4 (26%) had no major artery arising from FL, 5(33%) had 1 major artery arising from FL, 4(26%) had 2 major arteries arising from FL whereas 2(12%) had 3 arteries arising from FL.

Table 7 False lumen (FL) and true lumen(TL)characteristics

No of major vessels arising from FL	4(26%) had no arteries 5(33%) had 1 artery 4(26%) had 2 arteries 2(12%) had 3 arteries
FL size at LSCA in initial scan(mean)	24.8± 8.0 mm (7 mm-37 mm)
TL size at LSCA in initial scan(mean)	16.1 ±9.8 mm (7 mm- 37 mm)
FL size at D6 in initial scan(mean)	17.4 ±7.1mm (6 mm-29 mm)
TL size at D6 in initial scan(mean)	16.2 ±8.7 mm (7 mm-32 mm)
TL area (systolic)- at maximum diameter	383±300 mm ² (201-1104 mm ²)
FL areas(systolic)- at maximum diameter	630±478 mm ² (139-1374 mm ²)

2.4 Follow up

Follow-up scans showed growth in the overall aorta size and false lumen by an average of 5.1 mm and 3.6 mm respectively whereas there is not much growth (0.5 mm) in the true lumen. The average growth rate noticed in the present study is 5.12 mm/year (0 mm- 18 mm). Significant growth rate or enlarging aorta sizes were noticed in 5 (33%) patients whereas 10(66%) patients had stable growth (\leq 3 mm/year). Maximum growth was noted in the proximal DTA. Follow-up scans

showed patent lumen in nearly 93% (n=14) of cases among them 53% were completely patent, 40% partial thrombosed and only one patient (6%) had completely thrombosed FL.

Table 8 Follow-up details

Follow up details	
Maximum size of aorta follow-up scan(mean)	46.8± 8.0 mm (36 mm- 61 mm)
Average growth rate(mm/year)	5.12 (0 mm- 18 mm)
Enlarging aorta sizes (> 3 mm/y)	5(33%)
FL size at LSCA in follow-up scan(mean)	28.4± 9.4 mm (7 mm- 41 mm)
TL size at LSCA in follow-up scan(mean)	16.6 ±7.1 mm (8 mm- 38 mm)
FL size at D6 in follow-up scan(mean)	20.2 ± 8.1 mm (7 mm-31 mm)
TL size at D6 in follow-up scan(mean)	16.9 ±8.5 mm (8 mm-32 mm)
TL area (systolic)- at maximum diameter	390±310 mm ² (201-1204 mm ²)
FL areas(systolic)- at maximum diameter	680±488 mm ² (139-1674 mm ²)

The size of the false lumen increased in the follow-up scan as compared to the initial scan (mean false lumen size in the initial scan is 24.8 mm and in the follow-up scan is 28.4 mm) whereas the sizes of the true lumen are almost the same in the follow-up scan.

3. Relation of the expansion rate of the aorta to various demographic and anatomical parameters

Tests for normal distribution of the growth rate in millimeters were done which showed the data to be non-gaussian distribution (table 9). Hence nonparametric tests were done for evaluation of the correlation, regression, and hypothesis testing involving the rate of expansion of the aorta

Table 9 Statistical tests showing distribution of rate of expansion

	Statistics	p
Kolmogorov-Smirnov	0.35	.038
Kolmogorov-Smirnov (Lilliefors Corr.)	0.35	<.001
Shapiro-Wilk	0.73	.001
Anderson-Darling	1.89	<.001

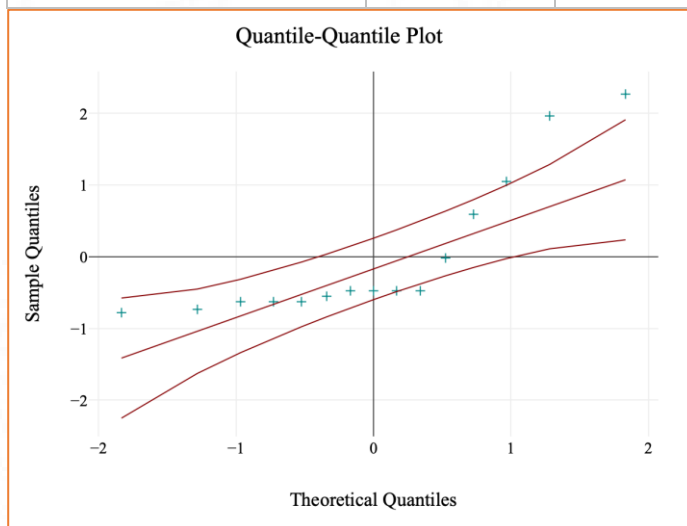


Figure 11 Scatter plot showing analysis of demographic and morphological parameter

3.1 Demographic results: Age, gender, presence of hypertension, diabetes, connective tissue disease, and smoking history was analyzed using Mann- Whitney U test which showed no statistical significance in the cases with enlarging aortic size compared to those with stable disease (Table 10).

Table 10 Demographic analysis

Demographics(n=15)	Stable (≤ 3 mm)(n=10)	Enlarging sizes >3 mm(n=5)	P value
Age	55.6 \pm 9.6	55.4 \pm 4.5	0.95
Sex	8(80%) males, 2(20%) females	4(80%) males, 1(20%) female	1.0
Hypertension	9(90%)	4(80%)	1.0
DM	2(20%)	0%	0.524
Smoking	2(20%)	2(40%)	0.56
Connective tissue disease	1(10%)	1(20%)	1.0
Uncontrolled HTN	3(30%)	0	0.505
Pulse rate \leq 70	8(80%)	5(100%)	0.524

3.2 Anatomical parameters:

Location of entry tear, the distance of entry tear, number of additional re-entry tears has no statistical significance in the present study. The patients with significant aortic growth had large entry tear size as compared to those with stable

disease and is of statistical significance (30% of the patients with stable disease had entry tear of less than 10 mm whereas almost all cases in enlarging aortic group had entry tear of more than 10 mm, $p=0.026$).

Table 11 Anatomical parameters analysis

Anatomical parameters	Stable (≤ 3 mm)(n=10)	Enlarging sizes >3 mm(n=5)	P value
No of the cases having ET >10 mm	3(30%)	5(100%)	0.026
Distance of ET from LSCA	14.9 \pm 14.5 mm	21.0 \pm 17.6 mm	0.197
Tear in inner wall of aorta	2(20%)	0	0.524
Number of additional tears in DTA-no	7(70%)	2(40%)	0.273
Number of additional tears in DTA-1	1(10%)	0	0.273
Number of additional tears in DTA-2	2(20%)	3(60%)	0.273
Growth rate(mm/year)	1.28 \pm 0.74	12.8 \pm 6.2	0.002

3.3 Correlation and regression analysis

A Spearman correlation done showed a medium, positive correlation between the size of entry tear and the growth rate in millimetre with $r= 0.41$ with no significant association between the size of entry tear and the growth rate in millimetre, $r= 0.41$, $p = 0. 131$. There was a low, positive correlation between the distance of the entry tear from the left subclavian artery and the growth rate in millimetre with $r= 0.19$ with no significant association between them $p = 0.488$. Spearman correlation showed a significant association between the growth rate in

millimetre and systolic false lumen areas $r = 0.62$, $p = 0.013$, and a high, negative correlation between the growth rate in millimeter and systolic true lumen area with $r = -0.5$.

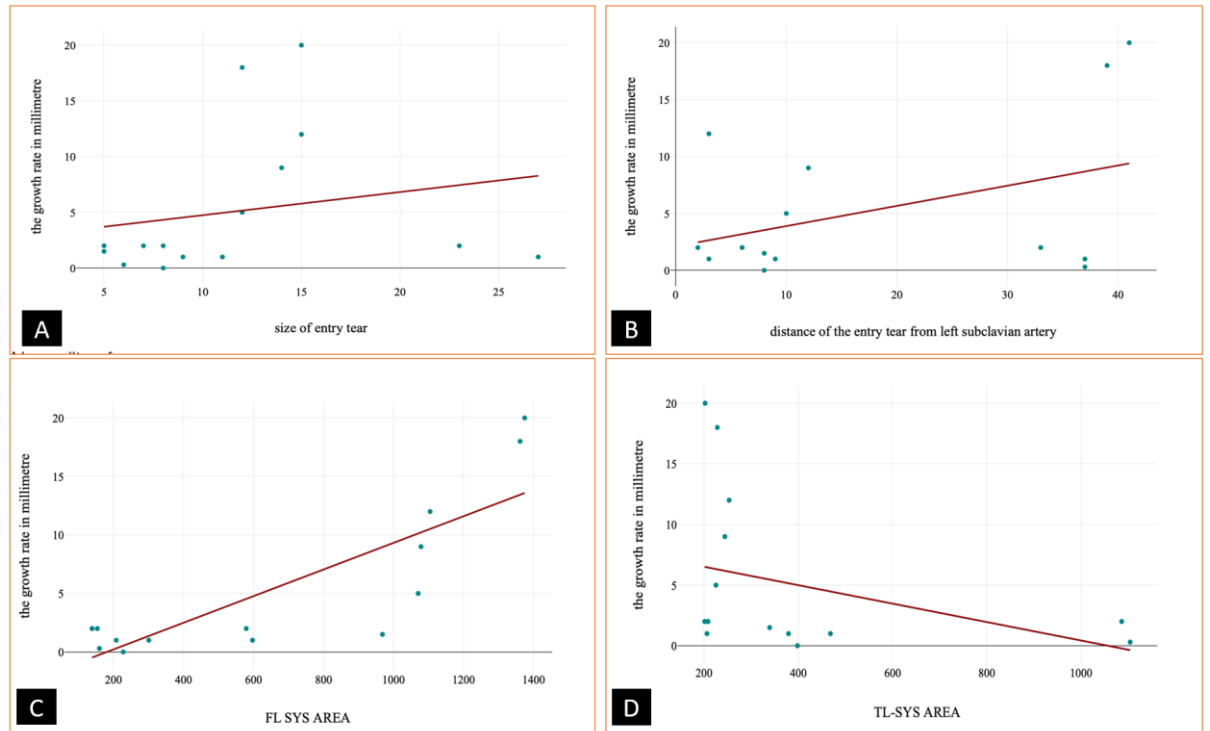


Figure 12 Scatter plot showing the relationship between growth rate and various morphological parameters

Image(A) shows relationship between growth rate and size of entry tear. Image (B) shows relationship between growth rate and distance of entry tear from left subclavian artery. Image(C) shows relationship between growth rate and false lumen systolic area. Image(D) shows relationship between growth rate and true lumen systolic area.

4. 4D Flow MRI parameters:

4.1 False lumen regurgitation fraction (FLRF)

In the present study, the overall false lumen regurgitation fraction for the 15 cases was $26.6 \pm 30.1\%$.

Among them, 5 cases with significant growth had a high false lumen regurgitation fraction of 64.8 ± 16.7 whereas the regurgitation fraction was significantly less in the cases with stable disease (7.6 ± 8.9). A Mann-Whitney U-Test showed that the difference between the two groups was statistically significant, $U=0$, $p=0.002$, $r=0.79$

Table 12 False lumen regurgitation fraction analysis

false lumen regurgitation fraction		N	Mean	Median	Standard deviation
Stable disease	0	10	7.63	4.3	8.92
Enlarging aorta sizes	1	5	64.8	72.6	16.75

Spearman correlation was performed to test whether there was an association between the growth rate in millimeter and false lumen regurgitation fraction. It showed that there was a significant association between the growth rate in millimeter and false lumen regurgitation fraction, $r(13) = 0.71$, $p = 0.003$

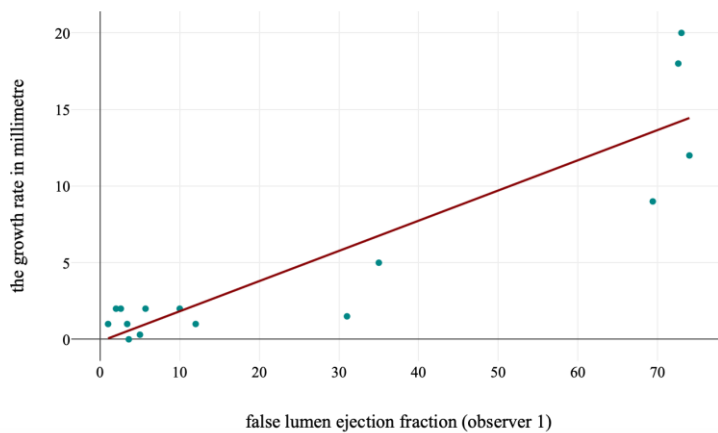


Figure 13 Scatter plot showing the correlation between growth rate and False lumen regurgitation fraction

Linear regression analysis showed false lumen regurgitation fraction explained 82.16% of the variance from the variable the growth rate in millimetre. it was found that the effect was significantly different from zero, $F=59.88$, $p < 0.001$, $R^2 = 0.82$

Energy loss in the DTA:

In the present study, overall energy loss in the DTA for the 15 cases was 1.81 ± 1.6 microwatts.

Among them, 5 cases with significant growth had high energy loss in the DTA of 2.2 ± 0.32 whereas energy loss was significantly less in the cases with stable disease 1.61 ± 1.99 microwatts. A Mann-Whitney U-Test showed that the difference was statistically significant, $U=5$, $p=0.014$, $r= 0.63$.

Table 13 Energy loss in the DTA analysis

Energy loss in the DTA		N	Mean	Median	Standard deviation
Stable disease	0	10	1.61	1.1	1.99
Enlarging aorta sizes	1	5	2.21	2.1	0.32

Spearman correlation was performed to test whether there was an association between the growth rate in millimeters and energy loss in the DTA. It showed that there was a significant positive association between the growth rate in millimeter and energy loss in the DTA, $r(13) = 0.56$, $p = 0.007$. There is a high, positive correlation between the variables the growth rate in millimetre and EL in the DTA with $r = 0.56$

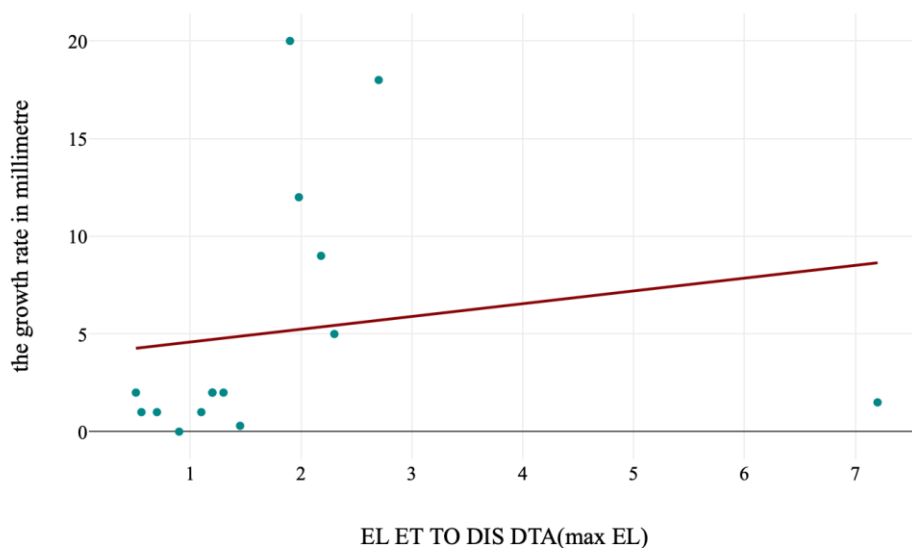


Figure 14 Scatter plot showing the correlation between growth rate and energy loss in the DTA

Linear regression analysis showed **the** percentage of EL in the DTA explained 2.64% of the variance from the variable the growth rate in millimeter. It

was found that the effect was not significantly different from zero, $F=0.35$, $p = 0.561$, $R^2 = 0.03$.

4.2 Percentage of energy loss in descending aorta:

In the present study, the overall percentage of energy loss in the DTA for the 15 cases was $47\% \pm 20\%$.

Among them, 5 cases with significant growth had a high percentage of energy loss in the DTA of $66\% \pm 17\%$ whereas energy loss was significantly less in the cases with stable disease of $37\% \pm 15\%$. A Mann-Whitney U-Test showed that the difference was statistically significant, $U=3$, $p=0.007$, $r= 0.7$.

Table 14 percentage of energy loss in the DTA analysis

percentage of energy loss in the DTA		N	Mean	Median	Standard deviation
Stable disease	0	10	37%	40%	15%
Enlarging aorta sizes	1	5	66%	58%	17%

Spearman correlation was performed to test whether there was association between the growth rate in millimeters and percentage loss of energy in the DTA. It showed that there was a significant association between the growth rate in millimeter and percentage loss of energy in the DTA, $r(13) = 0.62$, $p = 0.003$.

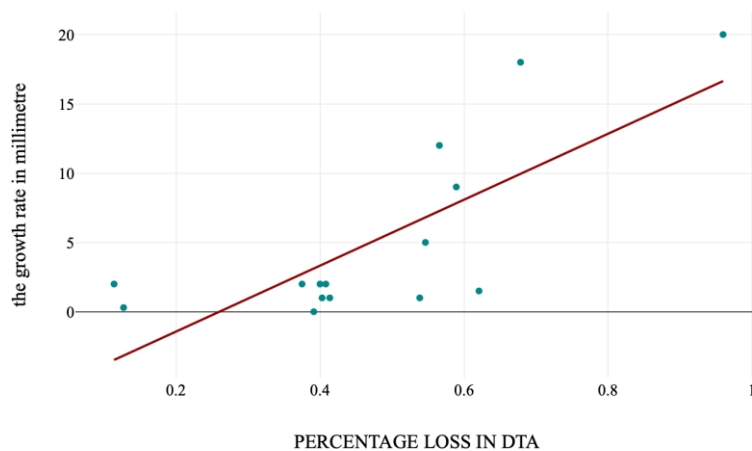


Figure 15 Scatter plot showing the correlation between growth rate and percentage energy loss in the DTA

Linear regression analysis showed **the** percentage of EL in the DTA explained 57.84% of the variance from the variable the growth rate in millimetre. It was found that the effect was significantly different from zero, $F=17.83$, $p = 0.001$, $R^2 = 0.58$.

4.3 Wall shear stress (WSS)

Wall shear stress was performed at various levels such as in the ascending aorta, true lumen, and false lumen within proximal 2 cm of the entry tear. In the ascending aorta, the maximum wall shear stress component was measured. In the true lumen and false lumen, axial and circumferential wall shear stress components were measured.

4.3.1. Circumferential wall shear stress of false lumen

In the present study, the overall circumferential WSS of the FL for the 15 cases was 0.11 ± 0.19 (Pa)

Among them, 5 cases with significant growth had higher circumferential WSS of the FL in the proximal DTA of 0.054 ± 0.016 whereas this was significantly less in the cases with stable disease 0.244 ± 0.314 . A Mann-Whitney U-Test showed the difference between the two groups was statistically significant, $U=9$, $p=0.047$, $r=0.51$.

Table 15 circumferential WSS of the FL(Pa) analysis

circumferential WSS of the FL(Pa)		N	Mean	Median	Standard deviation
Stable disease	0	10	0.054	0.050	0.016
Enlarging aorta sizes	1	5	0.244	0.15	0.314

Spearman correlation was performed to test whether there was an association between the growth rate in millimetre and circumferential WSS of the FL in the proximal DTA. It showed that there was a positive association between the growth rate in millimeter and circumferential WSS of the FL in the proximal DTA, $r = 0.46$, $p = 0.022$. There is a medium, positive correlation between the variables the growth rate in millimetre and circumferential WSS of the FL with $r = 0.46$.

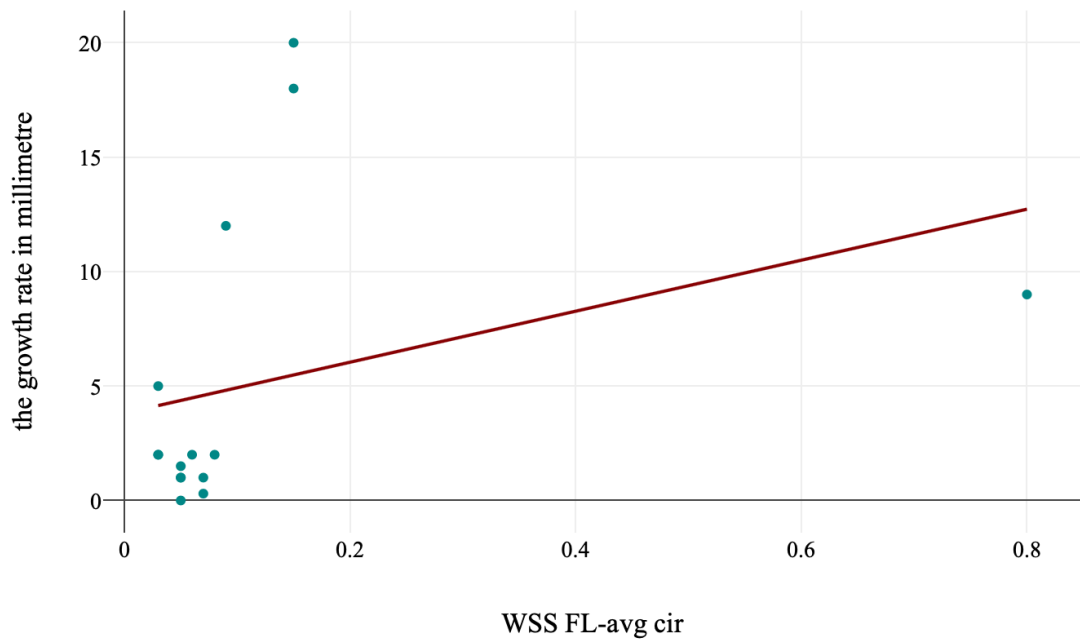


Figure 16 Scatter plot showing correlation between growth rate and circumferential wall shear stress of false lumen

Linear regression analysis showed circumferential WSS in the FL in the DTA explained 10.71% of the variance from the variable the growth rate in millimetre. It was found that the effect was not significantly different from zero, $F=1.56$, $p = 0.231$, $R^2 = 0.11$.

4.3.2. Circumferential wall shear stress of true lumen

In the present study, overall circumferential WSS of TL for the 15 cases was 0.11 ± 0.15 (Pa)

Among them, 5 cases with significant growth had higher circumferential WSS of the TL in the proximal DTA of 0.069 ± 0.02 Pa whereas this was less in the cases with stable disease 0.214 ± 0.25 . A Mann-Whitney U-Test showed that the

difference between the two groups was statistically significant, $U=6.5$, $p=0.022$, $r=0.59$.

Table 16 circumferential WSS of the TL(Pa)

circumferential WSS of the TL(Pa)		N	Mean	Median	Standard deviation
Stable disease	0	10	0.069	0.065	0.022
Enlarging aorta sizes	1	5	0.214	0.110	0.255

Spearman correlation was performed to test whether there was an association between the growth rate in millimeter and circumferential WSS of the TL in the proximal DTA. It showed that there was a significant positive association between the growth rate in millimeter and circumferential WSS of the TL in the proximal DTA, $r(13) = 0.56$, $p = 0.008$. There is a high, positive correlation between the growth rate in millimeter and circumferential WSS of TL with $r= 0.56$.

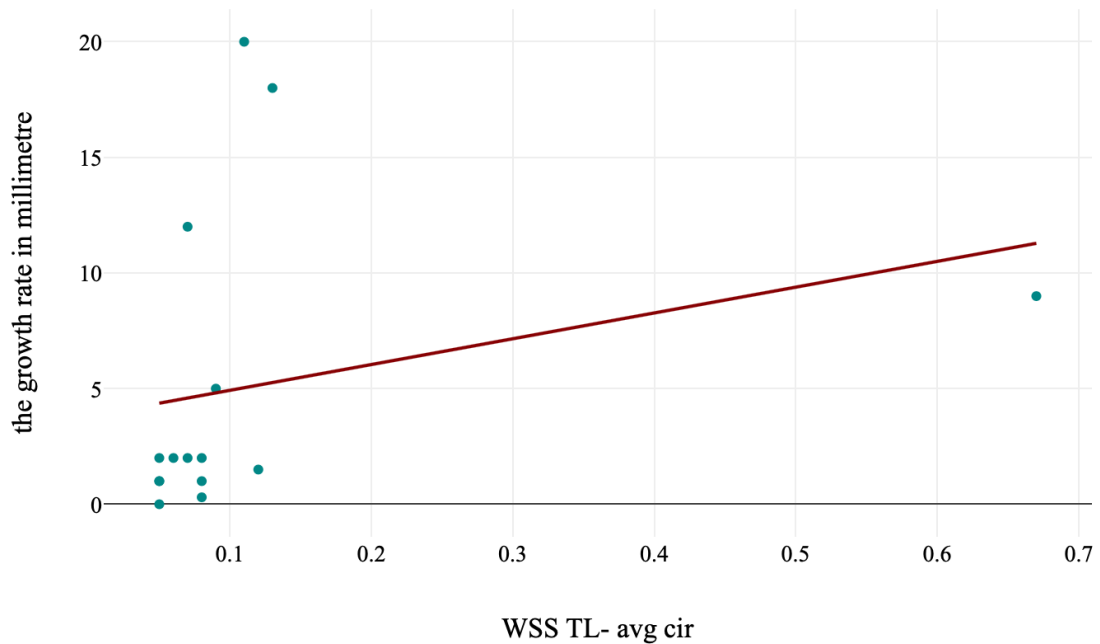


Figure 17 Scatter plot showing the correlation between growth rate and circumferential wall shear stress of true lumen

Linear regression analysis showed circumferential WSS in the TL in the DTA explained 6.95% of the variance from the variable the growth rate in millimetre. It was found that the effect was not significantly different from zero, $F=0.97$, $p = 0.34$, $R^2= 0.07$.

4.3.3. Wall shear stress of ascending aorta:

In the present study, overall circumferential WSS for the 15 cases was 0.18 ± 0.08 (Pa)

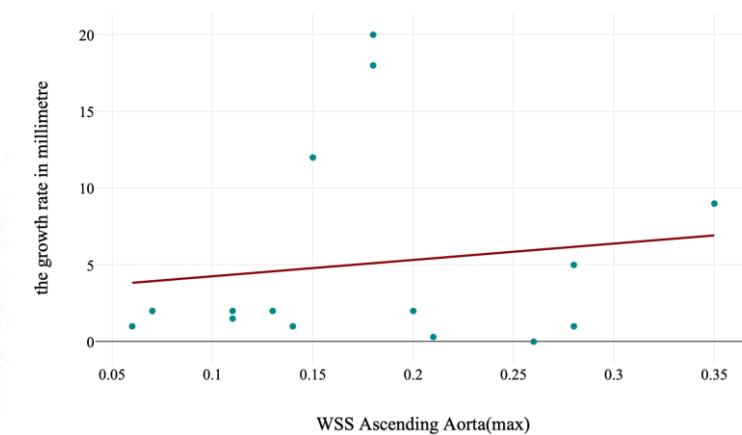
Among them, 5 cases with significant growth had higher ascending aorta WSS of 0.22 ± 0.08 whereas this was less in the cases with stable disease 0.15 ± 0.07 . A

Mann-Whitney U-Test showed the difference between the two groups was not statistically significant, $U=12.5$, $p=0.125$, $r= 0.4$.

Table 17 Max WSS of the ascending aorta (Pa) analysis

Max WSS of the ascending aorta (Pa)		N	Mean	Median	Standard deviation
Stable disease	0	10	0.1570	0.135	0.076
Enlarging aorta sizes	1	5	0.228	0.180	0.084

Spearman correlation was performed to test whether there was association between the growth rate in millimeter and the maximum WSS of the ascending aorta. It showed that there was no significant association between the growth rate in millimeter and WSS ascending aorta(max), $r = 0.06$, $p = 0.825$.



Normality of errors

Figure 18 Scatter plot showing the correlation between growth rate and wall shear stress of ascending aorta

Linear regression analysis showed maximum WSS of ascending aorta explained 1.84% of the variance from the variable the growth rate in millimetre. It was found that the effect was not significantly different from zero, $F=0.24$, $p = .628$, $R^2 = 0.02$.

4.3.4. Axial Wall shear stress of true lumen:

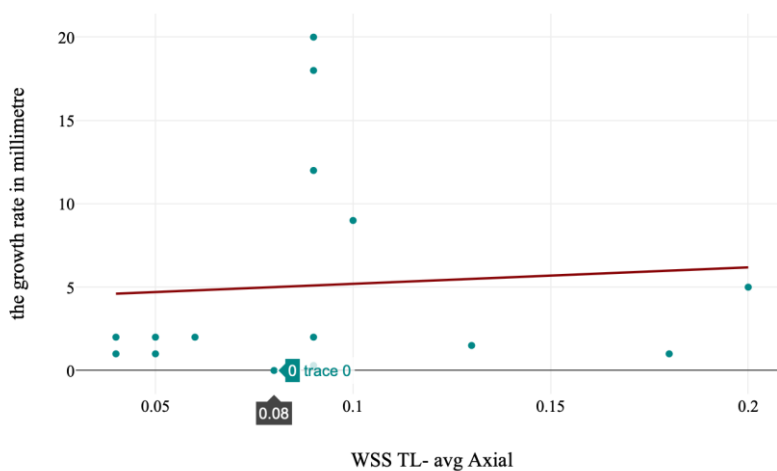
In the present study, the overall axial WSS of the TL for the 15 cases was 0.09 ± 0.04 (Pa)

Among them, 5 cases with significant growth had higher axial WSS of the TL in the proximal DTA of 0.114 ± 0.048 whereas this was less in the cases with stable disease 0.0810 ± 0.044 . A Mann-Whitney U-Test showed the difference between the two groups was not statistically significant, $U=20$, $p=0.538$, $r= 0.16$.

Table 18 Axial WSS of true lumen (Pa) analysis

Axial WSS of true lumen (Pa)		N	Mean	Median	Standard deviation
Stable disease	0	10	0.0810	0.07	0.044
Enlarging aorta sizes	1	5	0.114	0.09	0.048

Spearman correlation showed no significant association between the growth rate in millimetre and axial WSS of the TL, $r = 0.25$, $p = 0.378$. There is a low, positive correlation between the variables the growth rate in millimetre and axial WSS of TL with $r= 0.25$.



Normality of errors

Figure 19 Scatter plot showing the correlation between growth rate and axial wall shear stress of true lumen

Linear regression analysis showed axial WSS in the TL in the proximal DTA explained 0.5% of the variance from the variable the growth rate in millimetre. It was found that the effect was not significantly different from zero, $F=0.07$, $p = .801$, $R^2 = 0.01$.

4.3.5. Axial Wall shear stress of false lumen:

In the present study, the overall axial wall shear stress of false lumen for the 15 cases was 0.04 ± 0.019 (Pa)

Among them, 5 cases with significant growth had higher axial WSS of the FL in the proximal DTA of 0.064 ± 0.027 whereas this was less in the cases with stable disease 0.042 ± 0.007 . A Mann-Whitney U-Test showed that the difference between the two groups was not statistically significant, $U=11$, $p=0.077$, $r= 0.46$

Table 19 Axial WSS of False Lumen (Pa) analysis

Axial WSS of False Lumen (Pa)		N	Mean	Median	Standard deviation
Stable disease	0	10	0.042	0.04	0.078
Enlarging aorta sizes	1	5	0.064	0.06	0.027

Spearman correlation showed no significant association between the growth rate in millimetre and axial WSS of the FL, $r(13) = 0.4, p = 0.135$. There is a medium, positive correlation between the variables the growth rate in millimeter and axial WSS of FL with $r = 0.4$.

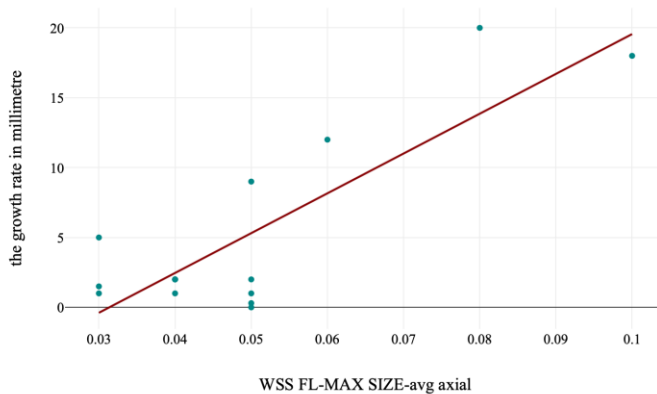


Figure 20 Scatter plot showing the correlation between growth rate and axial wall shear stress of false lumen

Linear regression analysis showed axial WSS in the FL in the proximal DTA explained 68.67% of the variance from the variable the growth rate in millimetre. it was found that the effect was significantly different from zero, $F=28.49, p < 0.001, R^2 = 0.69$.

4.4. Peak systolic velocity:

Peak systolic velocity was calculated in the true lumen and false lumen within 2 centimeters of the entry tear. The results were as follows:

4.4.1. Peak systolic velocity of the false lumen in the proximal DTA

In the present study, the overall mean peak systolic velocity in FL for the 15 cases was 67.9 ± 42.2 cm/s

Among them, 5 cases with significant growth had high PSV in the FL of 107 ± 54 cm/s whereas this was less in the cases with stable disease (48 ± 14 cm/s). A Mann-Whitney U-Test showed that the difference between the two groups with respect to PSV of FL was statistically significant, $U=8$, $p=0.037$, $r=0.54$

Table 20 PSV in False lumen in proximal DTA

PSV in False lumen in proximal DTA		N	Mean	Median	Standard deviation
Stable disease	0	10	48.4	52	14.3
Enlarging aorta sizes	1	5	107.0	87	54.2

Spearman correlation showed no significant association between the growth rate in millimetre and PSV in FL, $r(13) = 0.51$, $p = 0.055$. There is a high, positive correlation between the variables the growth rate in millimetre and PSV in FL with $r=0.51$.

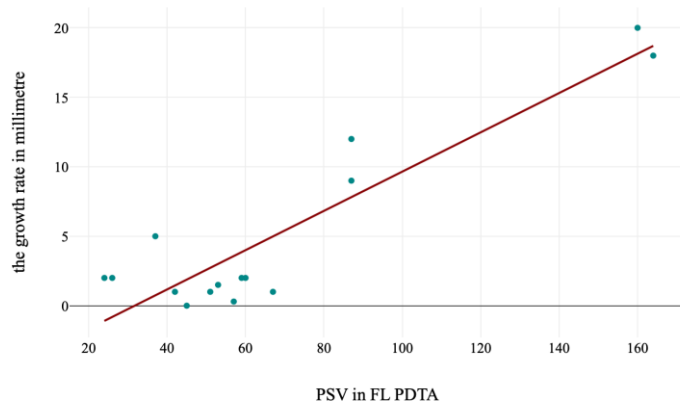


Figure 21 Scatter plot showing the correlation between growth rate and peak systolic velocity of the false lumen

Linear regression analysis showed PSV in FL explained 83.15% of the variance from the variable the growth rate in millimetre. It was found that the effect was significantly different from zero, $F=64.15$, $p = <0.001$, $R^2 = 0.83$.

4.4.1. Peak systolic velocity of the true lumen in the proximal DTA

In the present study, the overall mean peak systolic velocity in TL for the 15 cases was 111 ± 24.7 cm/s

Among them, 5 cases with significant growth had high PSV in the TL of 115 ± 39 cm/s whereas this was less in the cases with stable disease (109 ± 15). A Mann-Whitney U-Test showed that the difference between the two groups was not statistically significant, $U=20$, $p=0.54$, $r= 0.16$.

Table 21 PSV in True lumen in proximal DTA

PSV in True lumen in proximal DTA		N	Mean	Median	Standard deviation
Stable disease	0	10	109	115	15.8
Enlarging aorta sizes	1	5	115	141	39.3

Spearman correlation showed no significant association between the growth rate in millimetre and PSV in TL, $r(13) = 0.22$, $p = 0.109$. There is a low, positive correlation between the variables the growth rate in millimetre and PSV in TL with $r = 0.22$.

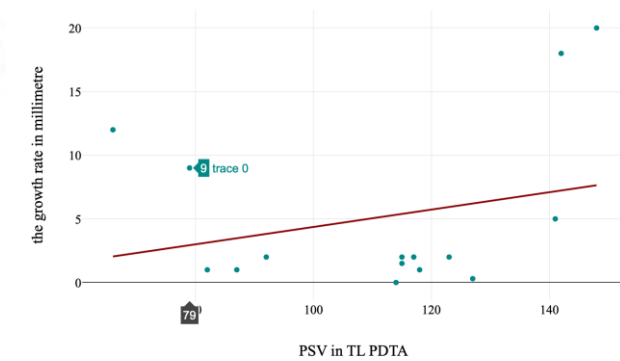


Figure 22 Scatter plot showing the correlation between growth rate and peak systolic velocity of true lumen

Linear regression analysis showed PSV in TL explained 6.64% of the variance from the variable the growth rate in millimetre. It was found that the effect was not significantly different from zero, $F=0.92$, $p = 0.352$, $R^2 = 0.07$.

4.5 Vortices

The vortical flow was seen in 86% (n=13) of the cases in the present study. Among them, 60% (n=9) had vortices of less than 360 degrees and 27% (n=4) had vortices of more than 360 degrees. Chi-Square test was performed to find whether high grade vortices result in significant growth. But it did not show statistically significant with a p value of 0.472.

5. **Multivariate analysis** was done to look for the association of significant growth rate with multiple parameters that showed significance in univariate analysis.

The circumferential TL-WSS was removed from the initial analysis and analyzed separately to prevent multicollinearity (VIF>10). The analysis showed FLRF and energy loss in DTA having independent predictors for the progression of dissection

Table 22 Multivariate analysis between various variables

	Unstandardized Coefficients	Standardized Coefficients			
Model	B	Beta	Standard error	t	p
(Constant)	-0.62		1.85	- 0.34	.742
false lumen regurgitation fraction (FLRF)	0.21	0.96	0.04	5.59	<0.001
Energy loss in DTA	-0.96	-0.24	0.43	- 2.25	.048

Circumferential WSS in false lumen (cWSS-FL)	-6.9	-0.2	4.01	-	.116
circumferential WSS TL	-9.05	-0.21	4.69	-	.082
Percentage energy loss in DTA	5.66	0.18	4.7	1.2	.256
R	R ²	Adjusted R ²	Standard error of the estimate		
0.95	0.91	0.88	2.31		

6. Reproducibility analysis / interobserver variation

The segmentation and analysis were done by 2 observers 3 years and 5 years experienced in cardiac MRI. The flow parameters are PSV in the true lumen, PSV in false lumen, and FLRF were compared between both observers. Interobserver variation was measured by Bland Altman plots

- a. **Peak systolic velocity of true lumen:** PSV was performed in true lumen in the proximal DTA by both the observers and Bland Altman plot was drawn which showed no significant interobserver variability.

Table 23 Interobserver variability related to PSV in TL

	PSV IN TL - Observer 1	PSV in TL Observer 2
Mean	109.73	111.07

Std. Deviation	22.35	24.76
Minimum	71	66
Maximum	139	148

Bland-Altman Plot

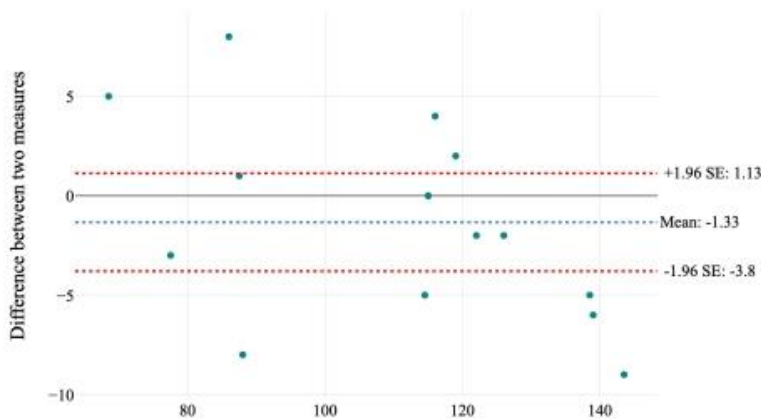


Figure 23 Bland Altman plot for PSV of true lumen between observer 1 and 2

- b. **Peak systolic velocity of false lumen:** PSV was performed in the false lumen in the proximal DTA by both the observers and Bland Altman plot was drawn which showed good agreement between two observers with no interobserver variability

Table 24 Interobserver variability related to PSV in FL

	PSV in FL (observer 1)	PSV in FL (observer 2)
Mean	65.07	67.93
Std. Deviation	38.76	42.3
Minimum	22	24

Maximum	158	164
---------	-----	-----

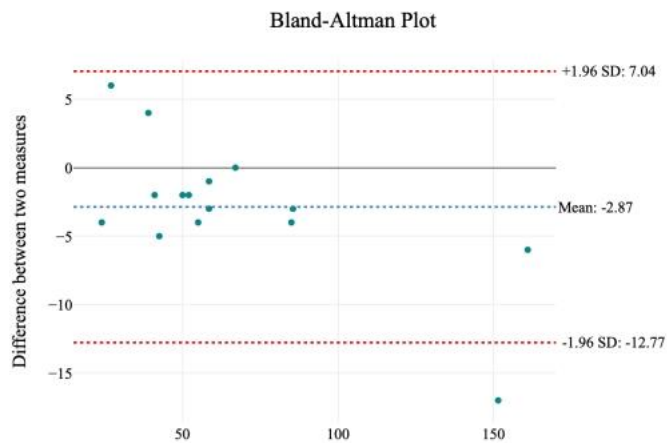


Figure 24 Bland Altman plot for PSV of false lumen between observer 1 and 2

- c. **False lumen regurgitation fraction (FLRF):** False lumen regurgitation fraction was performed in the false lumen in the proximal DTA by both the observers and Bland Altman plot was drawn which showed no significant interobserver variability.

Table 25 Interobserver variability related to false lumen regurgitation fraction

	false lumen regurgitation fraction (observer 1)	false lumen regurgitation fraction (observer 2)
Mean	26.69	26.29
Std. Deviation	30.16	29.8
Minimum	1	1

Maximum	74	73.2
Quartile 1	3.5	3.25
Skew	0.85	0.86
Kurtosis	-1.16	-1.14
95% Confidence interval of Mean	11.42; 41.95	11.21; 41.37
Mean \pm Std.	26.69 \pm 30.16	26.29 \pm 29.8

Bland-Altman Plot

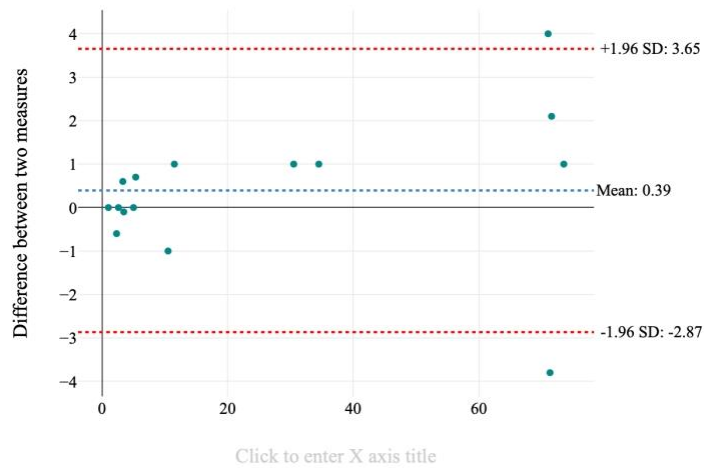


Figure 25 Bland Altman plot for FLRF between observer 1 and 2

Representative cases

Case 1 (Normal patient): 55-year-old male control patient.

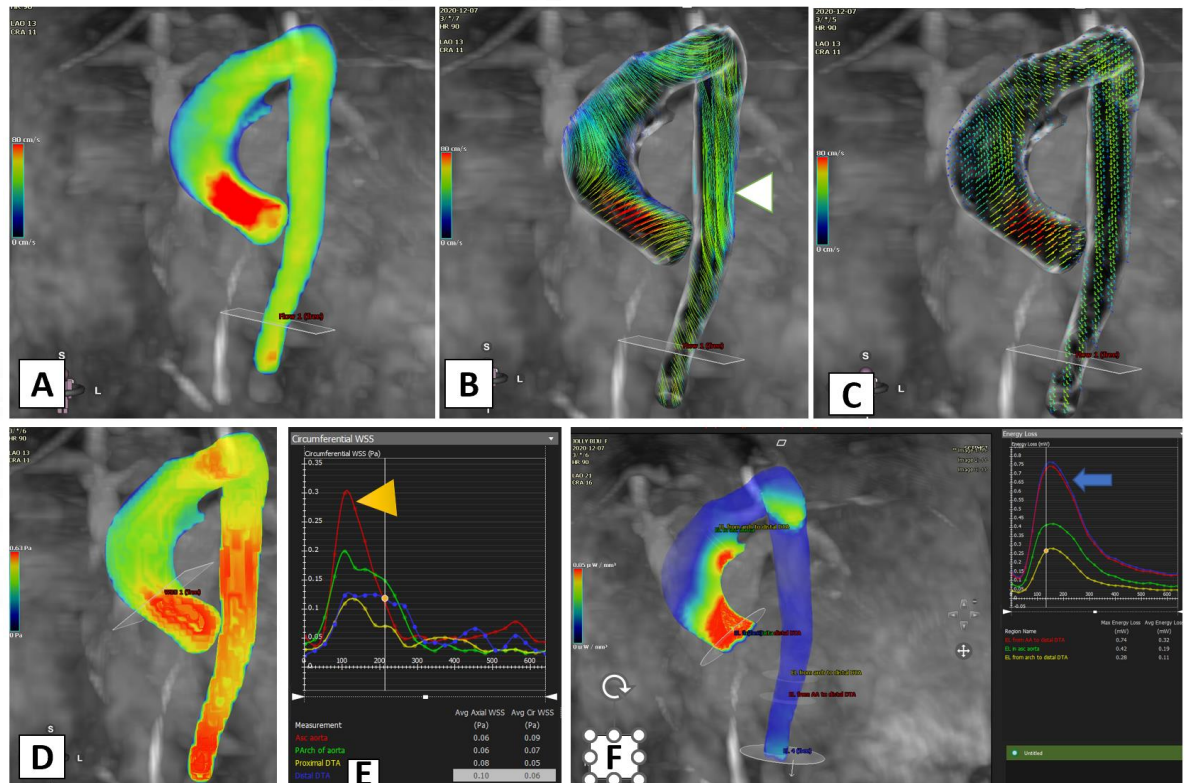


Figure 26 4D flow MRI images in a normal adult

4D flow images in normal healthy control of 55 years. Image (A) is showing velocity magnitude image with high velocity noted in the ascending aorta whereas rest of the aorta is not showing high velocity. Image (B) shows streamlines in normal aorta (arrowhead) which is showing laminar flow with high velocity at the center and low velocity at the periphery. Image (C) is showing vectors in which each vector shows the direction of the flow. Image (D) shows WSS in the aorta. Image (E) shows wall shear stress (WSS) at various locations. In the normal aorta highest circumferential WSS was noted in the ascending aorta. Image (F) shows energy loss

at various locations. In normal aorta, maximum energy loss is seen in ascending aorta with very less energy loss in DTA.

Case 2 (Rapidly expanding aorta)

61 year old male with history of CKD and HTN had follow-up MRI after 1 year.

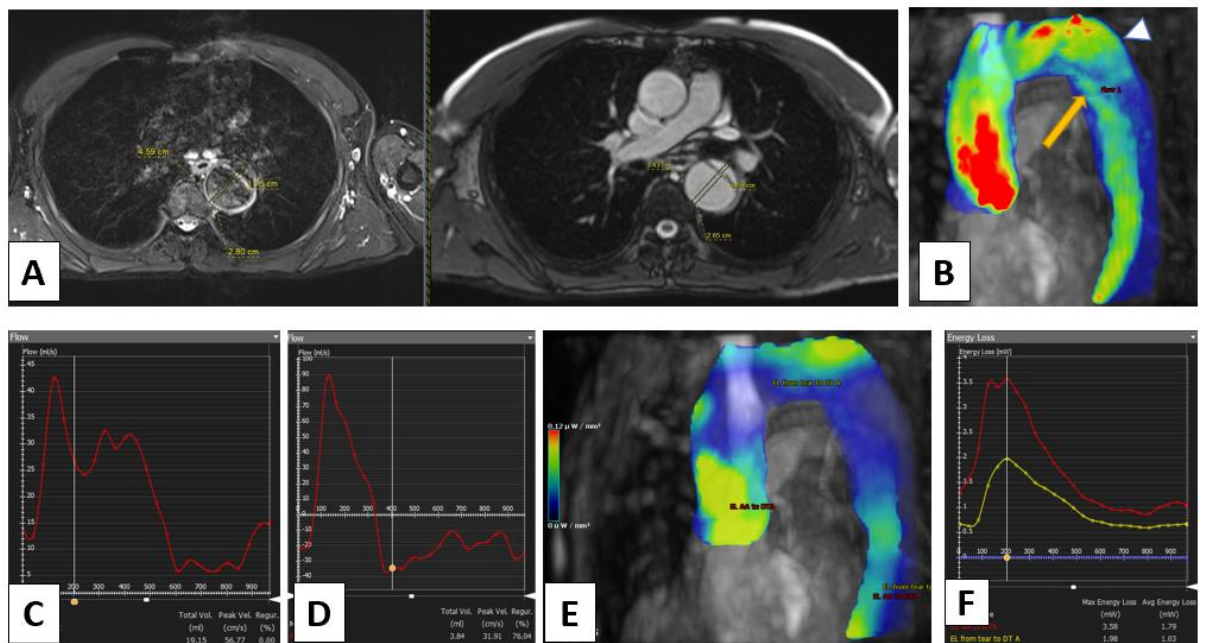


Figure 27 Case of the rapid expanding aorta in Type B AD patient

Image (A) double axial image in the proximal ascending aorta shows an increase in the size of the aorta of more than 12 mm over 1 year. Image (B): velocity magnitude image of aorta shows true lumen (arrow) and false lumen (arrowhead) with increased velocity at the entry tear and in the false lumen. Image (C): Peak systolic velocity (PSV) of the true lumen is 56 cm/s with no regurgitation fraction. Image (D): False lumen PSV of 32 cm/s with significant regurgitation of 76%. Image (E): Energy loss magnitude image shows energy loss in the ascending aorta and in the proximal DTA.

Image (F): values of energy loss(microwatt) with the percentage of energy loss in the DTA is 57%.

Case 3 (Rapidly expanding aorta)

51 year old male with history of HTN had rapid aortic growth of 20 mm over 1 year.

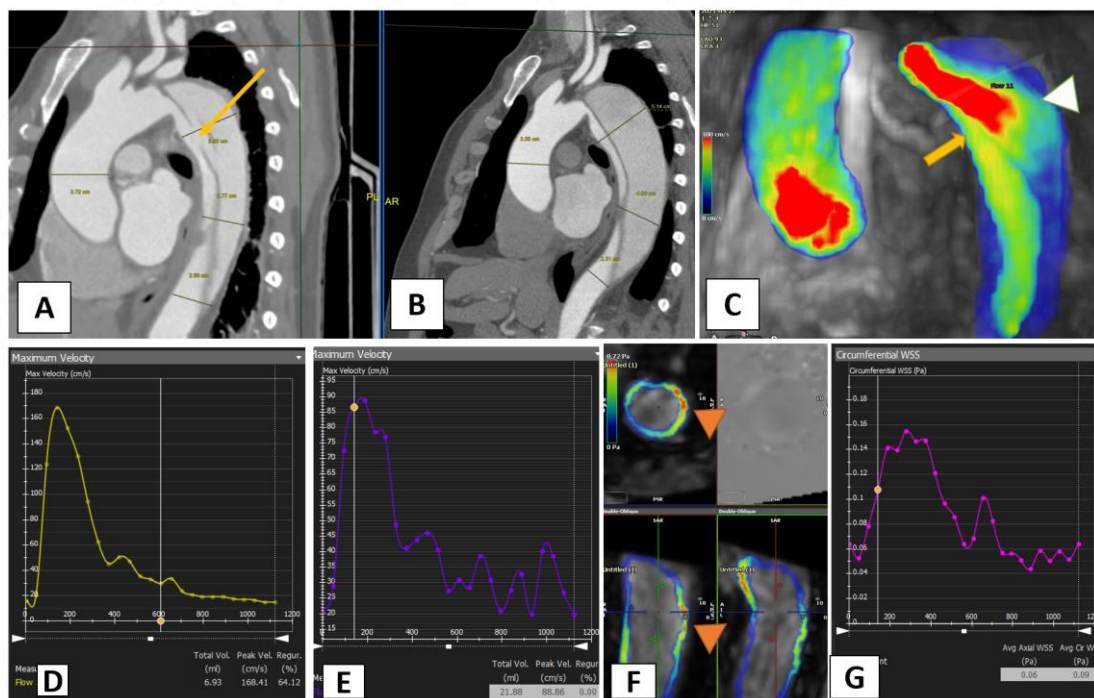


Figure 28 Case of rapidly expanding aorta in TBAD

Images (A) and (B) are the initial CT and follow-up CT images showed growth of approximately 20 mm in 1 year. He had an entry tear size of 15 mm at 40 mm from the left subclavian artery. Image (C)- velocity color-coded images shows significant high-velocity jet directed towards the false lumen. Peak systolic velocity in the false lumen is 168 cm/s and a regurgitation fraction of 64%. Image (E): True lumen flow at the same level shows PSV of 88 cm/s with no regurgitation fraction. Image (F):

MPR wall shear stress shows focal high WSS in the outer wall of the aorta. Image (G): shows increased circumferential WSS in the FL. This patient had a loss of 64% of energy in the DTA as compared to the whole aorta.

Case 4 (Stable aortic growth)

73 year old male with history of hypertension had aortic growth of 1-2 mm over 1 year.

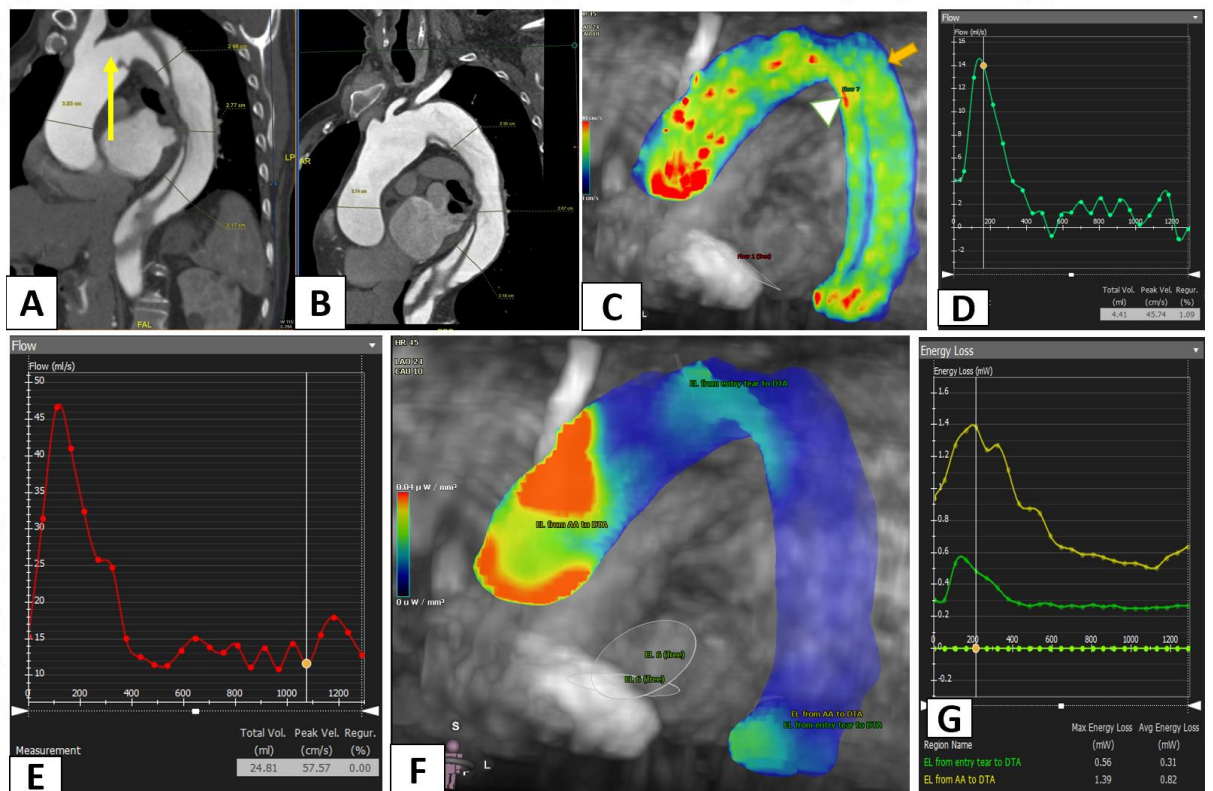


Figure 29 Patient with TBAD having stable growth

Images (A), (B) are the initial CT and follow-up CT images that showed a growth of approximately 1-2 mm in 1 year. He had an entry tear size of 15 mm (arrow in image A) immediately distal to left subclavian artery. Image (C)- velocity color-coded images show two separate lumens in the DTA with velocities near equal. Image (D): Peak systolic velocity in the FL is 45 cm/s and a regurgitation fraction of 2 %. Image E: TL flow at the same level shows PSV of 57 cm/s with no regurgitation fraction. Image (F): Magnitude image of energy loss which shows additional energy loss in the proximal DTA at the entry tear. Image (G): Values of viscous energy loss. This patient had a loss of 35% of energy in the DTA as compared to the whole aorta.

Case 5 (Stable aortic growth)

49 year old male with history of HTN had aortic growth of 1 mm over 1 year.

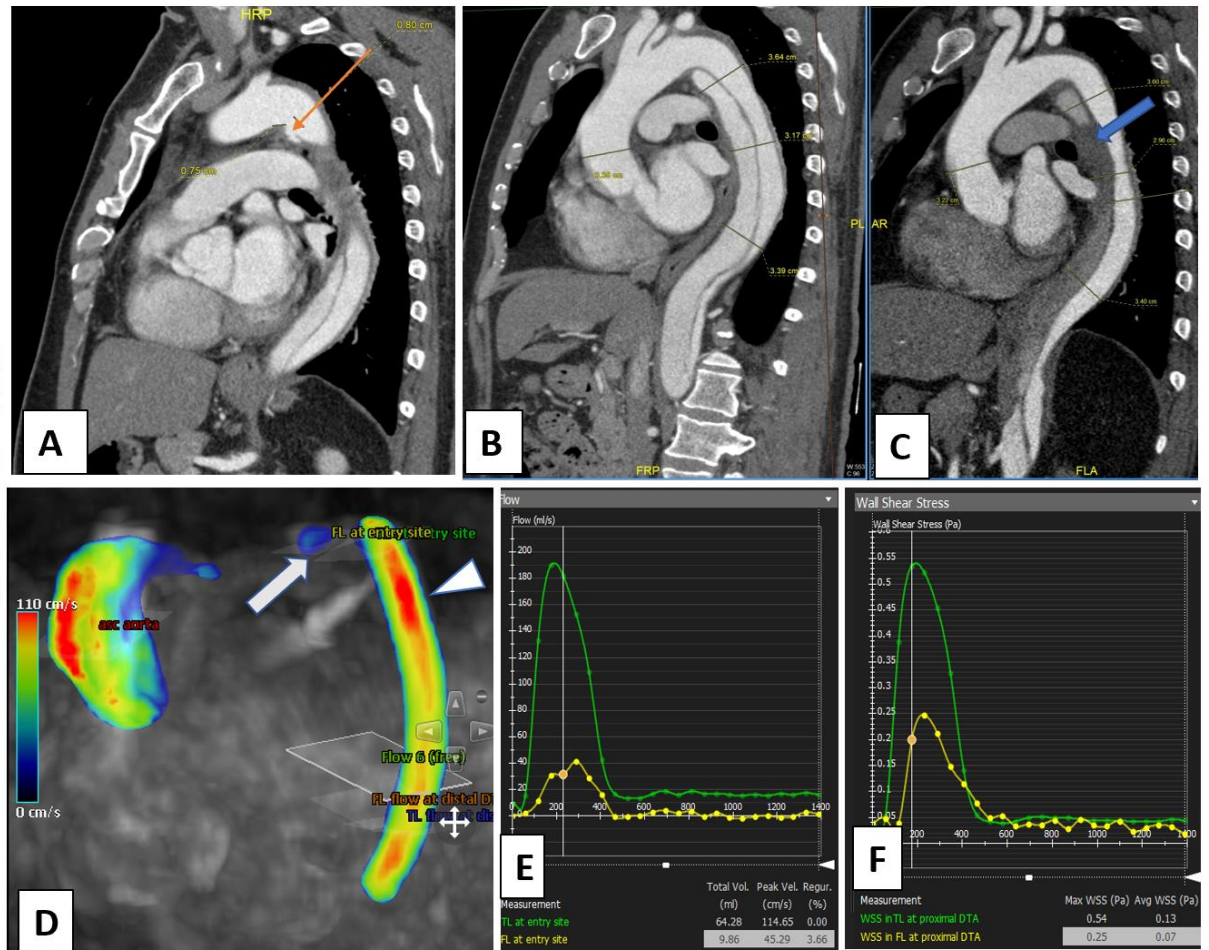


Figure 30 Case of TBAD with stable growth

65-year-old patient with Type B aortic dissection had an entry tear of size 8 mm on the inner aspect of aortic wall (orange arrow in image A). Image (B) CT scan at the time of index event and image (C) 1-year follow-up after index event showed no change in the sizes of aorta. Image (D)- 4D flow MRI magnitude image shows predominant flow into the true lumen (arrowhead) with very less flow in the false lumen (arrow). Corresponding velocity maps show low PSV as well as flow in the

false lumen at the entry site as compared to the true lumen with low regurgitation fraction from the false lumen. Even WSS values in the FL are less (image F). This patient had an energy loss of 36% in the DTA as compared to overall aorta.



Case 6 (Types of flow in 3 different patients)

Types of flow in 3 different patients:

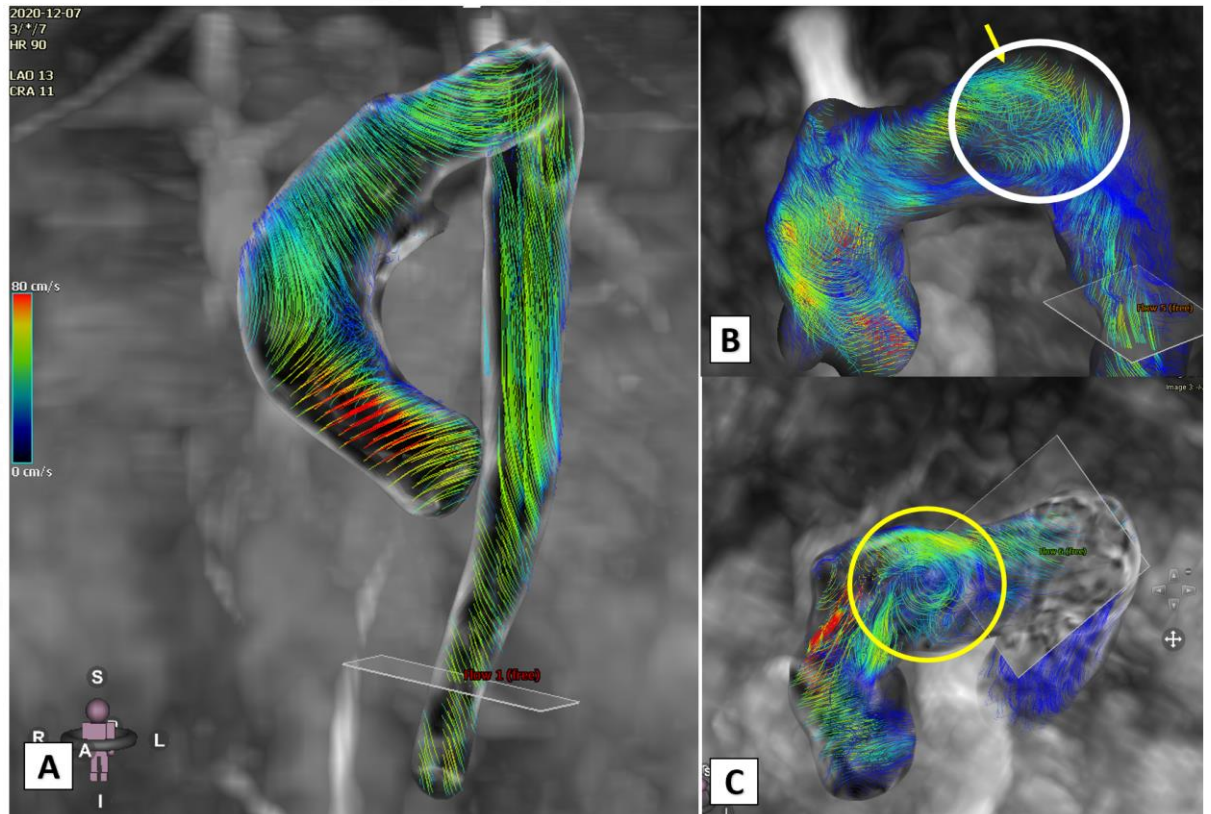


Figure 31 Flow patterns in 3 different patients

Image (A) in a normal patient shows laminar flow. Image (B) shows vortical flow at the ET site involving less than 360 degrees (white circle). Image (C) shows vortical flow at the ET site of more than 360 degrees (yellow circle)

5 DISCUSSION

Our prospective study done in 15 patients with uTBAD using 4Dflow MR and follow-up CT over 2 years showed the utility of 4D flow in predicting unstable dissections. Among the cohorts of 15, 5 cases had shown enlarging aortic sizes and 10 cases showed stable growth (≤ 3 mm/year). The results showed that the patient demographic including age, sex, presence of hypertension, diabetes, and collagen vascular disease has no significant correlation or association with expansion of dissection. Among the lesion characteristics size of the entry tear showed statistically significant difference between both the groups (stable disease vs enlarging aortic sizes) ($p=0.026$). Other parameters like the location of the ET on the inner wall of the aorta, distance of tear from LSCA, number of additional entry tears in the distal DTA, and number of arteries arising from false lumen did not show statistical significance between both groups

Among the 4D flow parameters, FLRF($p=0.002$), energy loss in the DTA($p=0.014$), percentage of energy loss in DTA (0.007), PSV in the FL ($p = 0.03$), circumferential WSS in the TL($p=0.022$) and FL ($p= 0.047$) showed statistically significant difference between stable disease versus enlarging aorta sizes. Positive association with growth rate was noted with parameters like FLRF ($r=0.71$, $p=0.003$), energy loss in the DTA ($r = 0.56$, $p = 0.007$), percentage of energy loss in DTA ($r = 0.62$, $p=0.013$), circumferential WSS in the FL $r = 0.46$, $p = 0.022$ and TL ($r = 0.56$, $p = 0.008$). No significant association was noted with parameters like PSV in FL ($r= 0.51$, $p = 0.055$). Multivariate analysis of these parameters showed that

FLRF($p < 0.001$) and energy loss in the DTA ($p = 0.048$) were independent predictors of the progression of the dissection (model adjusted $R^2 = 0.88$).

There is a gray zone regarding the treatment of uncomplicated type B aortic dissection (uTBAD) with no definite treatment guidelines to date. The proposed treatment is best medical management with serial cross-sectional imaging follow-up for monitoring size progression (MacGillivray et al., 2022). TEVAR or open surgical repair is recommended when there is rapid increase in the size of the aorta, size of aorta more than 55 mm, and symptomatic cases (MacGillivray et al., 2022). Complication rates remain high in uTBAD, with 25%–30% progressing toward complication within the first 14 days. Long-term outcomes are poor in medically managed patients with 30% of experience clinically significant aneurysmal degeneration in the first 4 years. Thus there has been increasing interest in the prophylactic management of uTBAD with TEVAR before complication onset. However, TEVAR itself carries risks such as retrograde type A dissection, stroke and paraparesis there is a necessity for appropriate risk stratification in patients with uTBAD. With the high reported number needed to treat (NTT) of 13 with TEVAR to prevent one aorta related mortality, a substantial opportunity for improved risk stratification and cost-effective care is needed which was attempted by our study. Direct flow measurements using 4D flow MRI was used to predict the patients who had rapid aortic growths.

In the present study, the overall false lumen regurgitation fraction for the 15 cases was $26.6 \pm 30.1\%$. Cases with significant growth had a high false lumen regurgitation fraction of $64.8 \pm 16.7\%$ whereas the regurgitation fraction was

significantly less in the cases with stable disease (7.6 ± 8.9). Our study results are consistent with Burriss et al, where in this prospective observational study in 18 patients having chronic descending aortic dissection (type B AD is 15 and repaired TAAD is 3) showed increased false lumen ejection fraction led to increased aortic growth in comparison with cases having stable disease (Burriss et al., 2019). However, our cohort were more homogenous (only Type B dissection) compared to Burriss et al. In addition, we didn't use any MRI contrast medium in our case. The segmentation was done from the magnitude images and thus obviated the need for contrast agent. To the best of our knowledge, there were no studies that were done without contrast agents.

Similar results were shown by Marlevi et al in 12 patients of chronic aortic dissection (11- TBAD, 1- repaired TAAD) using 4D flow MRI after giving contrast injection. Here patients with enlarging dissections have high FLEF as compared to stable disease ($49.0 \pm 17.9\%$ vs $10.0 \pm 11.9\%$, $p = 0.002$) (Marlevi et al., 2021). However, Marlevi used a retrospective group and the analysis of 4D flow was done in the chronic phase of dissection wherein expansion or remodeling has already set in. In our study 4D flow was done at the time (within 1 month of the event) and the cohort was followed up. In most of the studies in which 4D flow MRI was done in the chronic phase, there was scarce literature related to 4D flow in the subacute phase. This will be a better predictor of future expansion compared to the aforementioned study,

Spearman correlation significant association between the growth rate in millimeter and false lumen ejection fraction, $r(13) = 0.71$, $p = 0.003$. The correlation

between these can be explained by the higher retrograde flow across the FL in cases with increase in FL pressure (leading to high FLEF) (Burriss et al., 2019). Increased pressure in FL hinders continuous forward flow through the FL. During systole there will be forward flow due to high pressure in TL whereas during diastole as the pressure in TL falls, there will be more retrograde flow from the false lumen resulting in high regurgitation fraction from FL. Increased pressure in the FL leads to the rapid growth of the FL and aorta. This core physiology of the false lumen pressurization may be the cause where we found the FLRF to be an independent predictive factor for progression (($p < 0.001$) with an overall model adjusted $R^2=0.88$)

Our study showed that patients with significant growth had high energy loss in the DTA of 2.2 ± 0.32 compared to stable disease 1.61 ± 1.99 ($p=0.014$). An *ex vivo* computational hemodynamic evaluation in normal and diseased aorta (aneurysm, coarctation, and dissection) by Qiao et al. showed four sources of energy loss noted in the aorta which includes viscous friction, turbulence dissipation, wall deformation and local lesions. Among them, viscous friction of the blood leads to the excess amount of energy loss followed by aorta deformation(Qiao et al., 2022). However, there are very few studies related to viscous energy loss by 4D flow MRI with studies present in aortic stenosis rather than on aortic dissection.

A study on 16 patients having aortic dilation compared to 12 normal patients using 4D flow MRI by Barker et al showed significant viscous energy losses in the ascending aorta in patients with dilated aortas (2.2 ± 1.1 mW, $p=0.021$) and with aortic stenosis (10.9 ± 6.8 mW, $p < 0.001$) in comparison to healthy volunteers (1.2 ± 0.6 mW)(Barker et al., 2014). Jarvis et al studied kinetic energy in

20 patients with descending aortic dissection in comparison with 21 controls. They showed repaired TAAD had high TL kinetic energy(AAo repair: P = 0.021, ET1: P = 0.048), FL kinetic energy (AAo repair: P = 0.002, ET1: P = 0.024) and FL stasis (AAo repair: P = 0.003, ET1: P = 0.048) as compared to TBAD (Jarvis et al., 2020). However, they have not compared the expansion rates of uTBAD as done in our study.

In normal aortas, the loss of kinetic energy is more in ascending aorta. The percentage of energy loss in the DTA in the present study was 47%+/- 20%. The percentage amount of energy loss in the DTA in stable disease cases is 37%±15% and the percentage of energy loss in cases of significant growth is 66%±17%. Our cohort showed a excess energy loss in the DTA in expanding dissections. This excess energy loss in a particular segment results in the transfer of energy from the moving blood into the adjacent aorta wall leading to the rapid degeneration of the aortic wall resulting in aneurysmal growth(Qiao et al., 2022). The greater the energy loss makes the heart to work harder to compensate for the energy loss(Sträter et al., 2018). The more absolute energy loss in expanding dissection at the level of DTA implies force on the arterial wall resulting in expansion of the aorta which was evident in multivariate analysis (independent predictor for progression of disease (p= 0.048)). No studies to the best of our knowledge have shown the percentage loss of energy in DTA having an association with the progression of dissection.

In our study peak systolic velocity in the proximal false lumen was 67.9+/- 42.2 cm/s. PSV was higher in the cases with significant growth than those with stable disease (107±54 vs 48±14). P= 0.03, r= 0.54. with a high, positive correlation

between the PSV in FL and the growth rate with $r= 0.51$. A few studies have shown that high velocity and flow in the false lumen lead to the persistence of FL. Liu et al in 16 patients, showed large initial ET size correlated positively with average velocity, average net flow and peak flow in the false lumen($p<0.05$)(Liu et al., 2018). In another study by Shang et al in 14 patients having acute type B aortic dissection using CFD showed rapid aortic growth had high flow through false lumen compared to stable disease ($78.3\% \pm 9.3\%$ vs $56.3\% \pm 11.8\%$; $P = .016$)(Shang et al., 2015). High flow in the false lumen leads to the persistence of false lumen with less chance of thrombosis of false lumen. In the present study, there was larger entry site tear in the cases with significant growth, this large entry tear might cause high velocities in the false lumen in cases having significant growth.

Wall shear stress(WSS) is the tangential force applied by the moving blood on the wall of the aorta. High WSS leads to the initiation of dissection as well as degeneration of the extracellular matrix and elastic fibers. Low shear stress leads to thrombus formation of the false lumen(Pirola et al., 2019). Our study showed statistically significant difference in circumferential wall shear stress of false lumen and true lumen between stable and enlarging dissections. Study by Shang et al using CFD in 14 patients for assessment of TAWSS in type B AD patients, showed WSS on the aortic wall was higher in the cases with rapidly expanding aortic sizes (12.6 ± 3.7 vs 7.4 ± 2.8 Pa; $P = .028$). The same TAWSS for the entire aorta including aortic wall and dissection flap was not significant (Shang et al., 2015). The high wall shear stress in false lumen in our study is in line with previous studies. However, in our study it was not able to show the correlation in predicting aortic growth. The possible reason can be the previous studies used CFD for measuring WSS which has a high

spatial resolution in comparison to 4D flow and the 4D flow underestimates the values(Ferdian et al., 2021).

Our study found no significant correlation was noted between high-grade vortices and expansion of dissection (p-value 0.472). . In study on 32 patients with aortic dissection using multi VENC 4D flow MRI, Takahashi et al, showed that high amount of FL flow and velocity leads to higher vortex grade. Patients with more complication showed higher FL flow [41.7 (interquartile range, IQR 29.1–59.7) vs 17.7 (IQR 9.0–42.0) ml/s; P = 0.01], higher vortex grade [2 (IQR 1–2) vs 0 (IQR 0–2); P = 0.01] in comparison with stable disease(Takahashi et al., 2021). The possible reason for the vortical flow in the proximal FL is due to the acceleration of blood flow at the site of entry tear causing turbulence in the blood flow which results in spiral folding of the blood flow creating vortices. This recirculation of blood results in high-velocity jet imping focally on the wall(Saitta et al., 2021) which is a cause for negative remodeling of the aorta leading to expansion of false lumen and aorta(Takahashi et al., 2021). The discrepancy in the results of our study is difficult to explain and may be due to the low sample size in the present study and only few cases had significant growth

Strengths of the study

The present study is a prospective study with a homogenous group of population compared to other studies where both repaired TAAD and TBAD was evaluated as a single group. In addition, in our study the 4D flow was done in the early phase (within 1 month) and thus a better predictor for expansion compared to other studies where 4D flow was done in the chronic phase where the remodeling

and expansion has already occurred and only association can be obtained between the parameters. Our study used viscous energy loss compared to turbulent energy which was used in other study wherein energy loss over an aortic segment was calculated in our study (in comparison to previous studies where focal energy loss at a point was calculated,)thereby providing information related to entire aortic segment. Another strength is that in none of the cases MRI contrast agent was used for 4D flow MRI which is the greatest advantage in CKD patients. In addition we were able to provide multivariate analysis for the prediction of uTBAD which very few studies have addressed

Limitations:

Our sample size is modest. The reason for the small size is due to the low incidence of the disease. WSS assessed by the 4D flow MRI in the present study had low spatial resolution in comparison to CFD which was used in previous studies. In the present study, patients with connective tissue diseases(CTD) and those who do not have connective tissue diseases were assessed together which might affect the results due to the high growth rate and separate aortic wall shears in connective tissue disease.

To conclude 4D flow MRI can help in qualitatively as well as quantitatively assessing patients with uncomplicated type B aortic dissection. False lumen regurgitation fraction and the percentage amount of energy loss in DTA helps in predicting the growth of uncomplicated type B aortic dissection at an early stage. This will help to stratify those patients in the early phase who require early initiation

of endovascular treatment. However, we need studies with a larger sample size for generalization



6 SUMMARY AND CONCLUSIONS

In this single-center prospective observational study, a total of 15 patients were included in the study after excluding patients with type A AD, cTBAD, poor imaging quality and those who do not have follow-up. All 15 patients underwent 4D flow MRI within 1 month of initial CT angiography and follow-up CT angiography within 2 years to assess growth rate. Growth rate of more than 3 mm in one year is considered significant. These 15 patients were analyzed for flow parameters derived from 4D flow MRI in predicting aortic growth rate. In addition, demographic and anatomical parameters were also studied. Among 15 cases, 5 patients showed enlarging aortic sizes with the growth rate of more than 3 mm in one year and 10 patients had stable growth ($\leq 3\text{mm/year}$). Among the demographic and morphological parameters assessed, it is the entry tear size of more than 10 mm showed significant difference between cases with stable disease and enlarging group. It showed medium, positive correlation with the growth rate with $r = 0.41$ and no significant association between size of entry tear and the growth rate in millimeter, $r(13) = 0.41$, $p = 0.131$. Other morphological and anatomical parameters like age, gender, hypertension, smoking, diabetes mellitus, connective tissue disease, chronic kidney disease and morphological parameter's like the location of the ET on the inner wall of the aorta, distance of tear from LSCA, number of additional entry tears in the distal DTA and number of arteries arising from false lumen were not statistically different between cases with stable disease and significant growth. Among the 4D flow parameters, FLRF($p=0.002$), energy loss in the DTA($p=0.014$), percentage of energy loss in DTA (0.007), PSV in the FL ($p = 0.03$), circumferential

WSS in the TL($p=0.022$) and FL ($p= 0.047$) showed statistically significant difference between stable disease versus enlarging aorta group. Positive association with growth rate was noted with parameters like FLRF ($r=0.71$, $p=0.003$), energy loss in the DTA ($r = 0.56$, $p = 0.007$), percentage of energy loss in DTA ($r = 0.62$, $p=0.013$), circumferential WSS in the FL $r = 0.46$, $p = 0.022$ and TL($r = 0.56$, $p = 0.008$). No significant association was noted with parameters like PSV in FL ($r= 0.51$, $p = 0.055$). Multivariate analysis of these parameters showed FLRF($p<0.001$) and energy loss in the DTA ($p= 0.048$) are associated with independent predictors of the progression of the dissection with model adjusted $R^2=0.88$.

To conclude 4D flow MRI can help in qualitatively as well as quantitatively assessing patients with uncomplicated type B aortic dissection. False lumen regurgitation fraction and the viscous energy loss in DTA help in predicting the growth of uncomplicated type B aortic dissection at an early stage. This will help to stratify those patients in the early phase who require early initiation of endovascular treatment. However, we need studies with a larger sample size for generalization

7 REFERENCES

- Anagnostopoulos CE, Prabhakar MJ and Kittle CF (1972) Aortic dissections and dissecting aneurysms. *The American Journal of Cardiology* 30(3): 263–273. DOI: 10.1016/0002-9149(72)90070-7.
- Azarine A, Garçon P, Stansal A, et al. (2019) Four-dimensional Flow MRI: Principles and Cardiovascular Applications. *RadioGraphics* 39(3). Radiological Society of North America: 632–648. DOI: 10.1148/rg.2019180091.
- Barker AJ, van Ooij P, Bandi K, et al. (2014) Viscous Energy Loss in the Presence of Abnormal Aortic Flow. *Magnetic resonance in medicine : official journal of the Society of Magnetic Resonance in Medicine / Society of Magnetic Resonance in Medicine* 72(3): 620–628. DOI: 10.1002/mrm.24962.
- Booher AM, Isselbacher EM, Nienaber CA, et al. (2013) The IRAD classification system for characterizing survival after aortic dissection. *The American Journal of Medicine* 126(8): 730.e19–24. DOI: 10.1016/j.amjmed.2013.01.020.
- Burris NS, Nordsletten DA, Sotelo JA, et al. (2019) False lumen ejection fraction predicts growth in type B aortic dissection: preliminary results. *European Journal of Cardio-Thoracic Surgery : Official Journal of the European Association for Cardio-thoracic Surgery* 57(5): 896–903. DOI: 10.1093/ejcts/ezz343.
- Catapano F, Pambianchi G, Cundari G, et al. (2020) 4D flow imaging of the thoracic aorta: is there an added clinical value? *Cardiovascular Diagnosis and Therapy* 10(4): 1068–1089. DOI: 10.21037/cdt-20-452.
- Chen Y, Zhang S, Liu L, et al. (2017) Retrograde Type A Aortic Dissection After Thoracic Endovascular Aortic Repair: A Systematic Review and Meta-Analysis. *Journal of the American Heart Association* 6(9): e004649. DOI: 10.1161/JAHA.116.004649.
- Christoph A (n.d.) Endovascular Repair of Type B Aortic Dissection Long-term Results of the Randomized Investigation of Stent Grafts in Aortic Dissection Trial.
- Conzelmann LO, Weigang E, Mehlhorn U, et al. (2016) Mortality in patients with acute aortic dissection type A: analysis of pre- and intraoperative risk factors from the German Registry for Acute Aortic Dissection Type A (GERAADA). *European Journal of Cardio-Thoracic Surgery: Official Journal of the European Association for Cardio-Thoracic Surgery* 49(2): e44-52. DOI: 10.1093/ejcts/ezv356.
- Czerny M, Schmidli J, Adler S, et al. (2019) Editor's Choice - Current Options and Recommendations for the Treatment of Thoracic Aortic Pathologies Involving the Aortic Arch: An Expert Consensus Document of the European Association for Cardio-Thoracic Surgery (EACTS) & the European Society for Vascular Surgery (ESVS). *European*

Journal of Vascular and Endovascular Surgery: The Official Journal of the European Society for Vascular Surgery 57(2): 165–198. DOI: 10.1016/j.ejvs.2018.09.016.

- DeMartino RR, Sen I, Huang Y, et al. (2018) Population-Based Assessment of the Incidence of Aortic Dissection, Intramural Hematoma, and Penetrating Ulcer, and Its Associated Mortality From 1995 to 2015. *Circulation. Cardiovascular Quality and Outcomes* 11(8): e004689. DOI: 10.1161/CIRCOUTCOMES.118.004689.
- Evangelista A, Maldonado G, Grusso D, et al. (n.d.) Insights from the International Registry of Acute Aortic Dissection. *Global Cardiology Science & Practice* 2016(1): e201608. DOI: 10.21542/gcsp.2016.8.
- Fattori R, Montgomery D, Lovato L, et al. (2013) Survival after endovascular therapy in patients with type B aortic dissection: a report from the International Registry of Acute Aortic Dissection (IRAD). *JACC. Cardiovascular interventions* 6(8): 876–882. DOI: 10.1016/j.jcin.2013.05.003.
- Ferdian E, Dubowitz DJ, Mauger CA, et al. (2021) WSSNet: Aortic Wall Shear Stress Estimation Using Deep Learning on 4D Flow MRI. *Frontiers in Cardiovascular Medicine* 8: 769927. DOI: 10.3389/fcvm.2021.769927.
- Fleischmann D, Afifi RO, Casanegra AI, et al. (2022) Imaging and Surveillance of Chronic Aortic Dissection: A Scientific Statement From the American Heart Association. *Circulation: Cardiovascular Imaging* 15(3). American Heart Association: e000075. DOI: 10.1161/HCI.0000000000000075.
- Jarvis K, Pruijssen JT, Son AY, et al. (2020) Parametric Hemodynamic 4D Flow MRI Maps for the Characterization of Chronic Thoracic Descending Aortic Dissection. *Journal of Magnetic Resonance Imaging* 51(5): 1357–1368. DOI: 10.1002/jmri.26986.
- Liu D, Fan Z, Li Y, et al. (2018) Quantitative Study of Abdominal Blood Flow Patterns in Patients with Aortic Dissection by 4-Dimensional Flow MRI. *Scientific Reports* 8: 9111. DOI: 10.1038/s41598-018-27249-9.
- Lombardi JV, Hughes GC, Appoo JJ, et al. (2020) Society for Vascular Surgery (SVS) and Society of Thoracic Surgeons (STS) reporting standards for type B aortic dissections. *Journal of Vascular Surgery* 71(3): 723–747. DOI: 10.1016/j.jvs.2019.11.013.
- MacGillivray TE, Gleason TG, Patel HJ, et al. (2022) The Society of Thoracic Surgeons/American Association for Thoracic Surgery clinical practice guidelines on the management of type B aortic dissection. *The Journal of Thoracic and Cardiovascular Surgery* 163(4): 1231–1249. DOI: 10.1016/j.jtcvs.2021.11.091.
- Marlevi D, Sotelo JA, Grogan-Kaylor R, et al. (2021) False lumen pressure estimation in type B aortic dissection using 4D flow cardiovascular magnetic resonance: comparisons with aortic growth. *Journal of Cardiovascular Magnetic Resonance* 23: 51. DOI: 10.1186/s12968-021-00741-4.

- Melvinsdottir IH, Lund SH, Agnarsson BA, et al. (2016) The incidence and mortality of acute thoracic aortic dissection: results from a whole nation study. *European Journal of Cardio-Thoracic Surgery: Official Journal of the European Association for Cardio-Thoracic Surgery* 50(6): 1111–1117. DOI: 10.1093/ejcts/ezw235.
- Pirola S, Guo B, Menichini C, et al. (2019) 4-D Flow MRI-Based Computational Analysis of Blood Flow in Patient-Specific Aortic Dissection. *IEEE transactions on bio-medical engineering* 66(12): 3411–3419. DOI: 10.1109/TBME.2019.2904885.
- Qiao Y, Luo K and Fan J (2022) Component quantification of aortic blood flow energy loss using computational fluid-structure interaction hemodynamics. *Computer Methods and Programs in Biomedicine* 221: 106826. DOI: 10.1016/j.cmpb.2022.106826.
- Riambau V, Böckler D, Brunkwall J, et al. (2017) Editor’s Choice – Management of Descending Thoracic Aorta Diseases. *European Journal of Vascular and Endovascular Surgery* 53(1): 4–52. DOI: 10.1016/j.ejvs.2016.06.005.
- Rodríguez-Palomares JF, Dux-Santoy L, Guala A, et al. (2018) Aortic flow patterns and wall shear stress maps by 4D-flow cardiovascular magnetic resonance in the assessment of aortic dilatation in bicuspid aortic valve disease. *Journal of Cardiovascular Magnetic Resonance: Official Journal of the Society for Cardiovascular Magnetic Resonance* 20(1): 28. DOI: 10.1186/s12968-018-0451-1.
- Ruiz-Muñoz A, Guala A, Dux-Santoy L, et al. (2022) False lumen rotational flow and aortic stiffness are associated with aortic growth rate in patients with chronic aortic dissection of the descending aorta: a 4D flow cardiovascular magnetic resonance study. *Journal of Cardiovascular Magnetic Resonance: Official Journal of the Society for Cardiovascular Magnetic Resonance* 24(1): 20. DOI: 10.1186/s12968-022-00852-6.
- Sailer AM, van Kuijk SMJ, Nelemans PJ, et al. (2017) Computed Tomography Imaging Features in Acute Uncomplicated Stanford Type-B Aortic Dissection Predict Late Adverse Events. *Circulation: Cardiovascular Imaging* 10(4). American Heart Association: e005709. DOI: 10.1161/CIRCIMAGING.116.005709.
- Saitta S, Guo B, Pirola S, et al. (2021) Qualitative and Quantitative Assessments of Blood Flow on Tears in Type B Aortic Dissection With Different Morphologies. *Frontiers in Bioengineering and Biotechnology* 9: 742985. DOI: 10.3389/fbioe.2021.742985.
- Shang EK, Nathan DP, Fairman RM, et al. (2015) Use of computational fluid dynamics studies in predicting aneurysmal degeneration of acute type B aortic dissections. *Journal of vascular surgery* 62(2): 279–284. DOI: 10.1016/j.jvs.2015.02.048.
- Sträter A, Huber A, Rudolph J, et al. (2018) 4D-Flow MRI: Technique and Applications. *RoFo: Fortschritte Auf Dem Gebiete Der Rontgenstrahlen Und Der Nuklearmedizin* 190(11): 1025–1035. DOI: 10.1055/a-0647-2021.

- Sueyoshi E, Sakamoto I, Hayashi K, et al. (2004) Growth rate of aortic diameter in patients with type B aortic dissection during the chronic phase. *Circulation* 110(11 Suppl 1): II256-261. DOI: 10.1161/01.CIR.0000138386.48852.b6.
- Takahashi K, Sekine T, Miyagi Y, et al. (2021) Four-dimensional flow analysis reveals mechanism and impact of turbulent flow in the dissected aorta. *European Journal of Cardio-Thoracic Surgery: Official Journal of the European Association for Cardio-Thoracic Surgery* 60(5): 1064–1072. DOI: 10.1093/ejcts/ezab201.
- Tolenaar JL, van Keulen JW, Jonker FHW, et al. (2013) Morphologic predictors of aortic dilatation in type B aortic dissection. *Journal of Vascular Surgery* 58(5): 1220–1225. DOI: 10.1016/j.jvs.2013.05.031.
- Tolenaar JL, van Keulen JW, Trimarchi S, et al. (2013) Number of Entry Tears Is Associated With Aortic Growth in Type B Dissections. *The Annals of Thoracic Surgery* 96(1): 39–42. DOI: 10.1016/j.athoracsur.2013.03.087.
- Tolenaar JL, Froehlich W, Jonker FHW, et al. (2014) Predicting in-hospital mortality in acute type B aortic dissection: evidence from International Registry of Acute Aortic Dissection. *Circulation* 130(11 Suppl 1): S45-50. DOI: 10.1161/CIRCULATIONAHA.113.007117.
- Tsai TT, Fattori R, Trimarchi S, et al. (2006) Long-Term Survival in Patients Presenting With Type B Acute Aortic Dissection. *Circulation* 114(21). American Heart Association: 2226–2231. DOI: 10.1161/CIRCULATIONAHA.106.622340.
- Xiang D, Kan X, Liang H, et al. (2021) Comparison of mid-term outcomes of endovascular repair and medical management in patients with acute uncomplicated type B aortic dissection. *The Journal of Thoracic and Cardiovascular Surgery* 162(1): 26-36.e1. DOI: 10.1016/j.jtcvs.2019.11.127.

ANNEXURES

List of publications from Thesis


Nil



Curriculum Vitae

CV of the Investigator

BELLALA	AJAY PAVAN	KUMAR
Last Name	First Name	Middle Name
Date of Birth (dd/mm/yy) 27-06-1993		Sex male
Study Site Affiliation (e.g. Principal Investigator, Co-Investigator, Coordinator): Principal Investigator		
Professional Mailing Address (Include Institution name)	Study Site Address (Include Institution name)	
Senior resident, department of IS IR, SCTIMST, TVM	Senior resident, department of IS IR, SCTIMST, TVM	
Telephone (Office):	Mobile Number: 9573970897	
Telephone (Residence):	Email: bellala.ajaypavankumar@gmail.com	
Academic Qualifications (Most recent qualification first)		
Degree/Certificate	Year	Institution, Country
MD, RADIODIAGNOSIS	2019	OSMANIA MEDICAL COLLEGE, HYD,INDIA

MBBS	2016	GANDHI MEDICAL COLLEGE, HYD,INDIA
Details of professional registration : (MCI/State Registration/Bar Council/DCI/etc including Registration Number and Year of Registration TSMC/FMR/00525, YEAR-2016		
Current and previous positions (most recent position first)		
Month and Year	Title	Institution/Company, Country
Brief summary of relevant research experience:		
NIL		
Current project/s at hand:		
NIL		
 Signature:		Date:29-7-2022 Place:TRIVANDRUM

CV of the Investigators

Last Name- valakkada	First Name- Jineesh	Middle Name
Date of Birth (dd/mm/yy) 17/04/1987		Sex M

Study Site Affiliation (e.g. Principal Investigator, Co-Investigator, Coordinator) Co- Principal Investigator

Professional Mailing Address (Include Institution name)	Study Site Address (Include Institution name)
Assistant Professor Department of IS& IR, SCTIMST, Trivandrum Kerala- 695011	Department of IS& IR, SCTIMST, Trivandrum Kerala- 695011
Telephone (Office):	Mobile Number: 8447284059
Telephone (Residence):	Email: jineesh174@gmail.com

Academic Qualifications (Most recent qualification first) MD RadioDiagnosis, MBBS

Degree/Certificate	Year	Institution, Country
Fellowship GI intervention radiology	2017	AIIMS – NEWDELHI
MD radiodiagnosis	2013	AIIMS- NEWDELHI
DNB RADIODIAGNOSIS	2014	

Details of professional registration: (MCI/State Registration/Bar Council/DCI/etc including Registration Number and Year of

Registration TCMC- 44903

Current and previous positions (most recent position first)

Month and Year	Title	Institution/Company, Country
2018 FEB- present	Assistant professor –IS and IR	SCTIMST- TRIVANDRUM
2014-2017	Senior resident	AIIMS – NEWDELHI

Publications:.

Valakkada J, Chandran R, Mishra P, Pawar DK, Maitra S,. Internal jugular vein thrombosis from rhino-cerebral mucormycosis: a case report. Internal medicine. 2014 Aug;53(8):1185-9.
careful before cannulation. Indian J Crit Care Med Peer-Rev Off Publ Indian Soc Crit Care Med. 2014 Aug

Kumar V, Karunakaran A, Valakada J. Septo-optic dysplasia. Int Ophthalmol. 2017 Jan 3

Jineesh, Gamanagatti S, Rangarajan K, Kumar A,. Blunt abdominal trauma: imaging and intervention. Curr Probl Diagn Radiol. 2017 Aug;44(4):321–36. 4. Abdominal lymphangiomatosis with intestinal lymphangectasia – MR lymphangiography (CDPR)

primary cutaneous histoplasmosis with splenic involvement

salpingocolic fistula – case report 2017

salpingocolic fistula – case report 2017

Current project/s at hand: 1.IVIM in hepatocellular carcinoma

2.Prophylactic ballooning in radiocephalic fistulas- RCT

A	Anoop	
Last Name	First Name	Middle Name
Date of Birth (dd/mm/yy) 03/11/86		Sex Male
Study Site Affiliation (e.g. Principal Investigator, Co-Investigator, Coordinator) Principal Investigator		
Professional Mailing Address (Include Institution name)		Study Site Address (Include Institution name)
Assistant professor Department of IS& IR, SCTIMST, Trivandrum Kerala- 695011		Assistant professor Department of IS& IR, SCTIMST, Trivandrum Kerala- 695011
Telephone (Office): 04712524220		Mobile Number: 8547683011
Telephone (Residence):		Email: anoop.a@sctimst.ac.in
Academic Qualifications (Most recent qualification first) PDCC. MD RadioDiagnosis, MBBS		
Degree/Certificate	Year	Institution, Country
PDCC in vascular interventions and cardiac imaging	2015	Sree Chitra Tirunal Institute for Medical Sciences & Technology, Trivandrum
MD (Radio-Diagnosis) Doctor of Medicine	2014	Institute Of Post Graduate Medical Education And Research & SSKM hospital, Kolkata.

MBBS	2010	Govt . medical college, Kozhikode, Kerala
Details of professional registration : (MCI/State Registration/Bar Council/DCI/etc including Registration Number and Year of Registration - TCMC no: 42911 of 2011		
Current and previous positions (most recent position first)		
Month and Year	Title	Institution/Company, Country
July 2017	Assistant Professor, IS & IR	SCTIMST
Jan 2016	Assistant Professor(Ad hoc), IS & IR	SCTIMST
Brief summary of relevant research experience: Have got intramural and extramural funding for few unique projects and are in the process of completion		

Current project/s at hand:

Role of non-contrast and post contrast myocardial T1 mapping in hypertrophic and dilated cardiomyopathy-IEC approved no: SCT/ IEC/856/feb2016.

Three-dimensional printing in congenital heart disease- Jun2018-jun2021 in SERB, Govt of India. SCT/ IEC/1076/dec2017.

Assessment of carotid plaque vulnerability using 3T MRI & correlation with carotid endarterectomy- TDF funded approved project, 2-year duration–October 2018-2020. SCT/ IEC/1239/aug2018.

[Handwritten signature]

Signature:

Date: 27-6-19

Place: Thiruvananthapuram



		SHIVANESAN	
Last Name	First Name		N
(/mm/yy) 14/8/1985.		Sex	MALE
CO-INVESTIGATOR			
() Dept of C S SCTIMST, Trivandrum		() Dept of TS, SCTIMST, Trivandrum	
p ():		70425	
p ():		Email drpshivanesan@gmail.com	
Qualifications ()			
Degree/		Institution, Country	
MCh VASCULAR SURGERY	2017	SCTIMST, Trivandrum	
MS Gen Surgery	2013	PGIMER, Chandigarh	
86582.			
previous p () position first			
		Institution/Company, Country	
2017	Asst. Professor	SCTIMST, Trivandrum	
Signature: <i>[Signature]</i>		Date:	Place: Trivandrum

V2.15042017

The following members of the Students Sub-Committee of the Institutional Ethics Committee participated in the discussions held on Dec 9, 2020 at the offices and residences of the members

SL. No.	Member Name	Highest Degree	Gender	Scientific /Non Scientific	Affiliation with Institution(s)
1.	Dr. R V G Menon	M Tech, PhD	Male	Lay Person (Chairman)	No
2.	Dr. Harikrishnan S	MD, DM (Cardiology) DNB (Cardiology)	Male	Clinician	Yes
3.	Dr. Kala Kesavan. P	MBBS, MD	Female	Basic Medical Scientist	No
4.	Dr. Rema M. N	MD	Female	Basic Medical Scientist	No
5.	Dr. Christina George	MD Psychiatry	Female	Clinician	No
76	Dr. Mala Ramanathan	PhD	Female	Social Scientist (Member Secretary)	Yes

IEC Decision

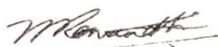
The IEC approved the conduct of the study in the present form.

Remarks:

The Institutional Ethics Committee expects to be informed about the progress of the study, any SAE occurring in the course of the study, any changes in the protocol and patient information/informed consent and asks to be provided a copy of the final report.

There was no member of the study team who participated in voting / decision making process. The ethics committee is organized and operated according to the requirements of Good Clinical Practice and the requirements of the Indian Council of Medical Research (ICMR).

Sincerely,



Mala Ramanathan
Member Secretary, IEC

APPENDIX B – SUPPLEMENTARY TABLES

TITLE: Qualitative and quantitative assessment of hemodynamic parameters by 4D flow MRI in uncomplicated descending (type B) aortic dissection.

Age:

Sex:

Clinical details

Clinical details	
Age	Connective tissue disease
Sex	Blood pressure at the time of MRI
Hypertension	Controlled/uncontrolled hypertension
Diabetes mellitus	Pulse rate
Smoking	Chronic kidney disease (CKD)

Morphological details from imaging

CT angiographic parameter assessment
Ascending aorta size
Size of entry tear, Location of entry tear from LSCA
Size of true lumen, false lumen, aorta size within 2 cm from LSCA, at D6 levels, Hiatus level, at maximum size in DTA

No of re-entry tears in DTA
No of arteries arising from false lumen

4D flow MRI parameters

Qualitative parameters	Quantitative parameters
Streamlines to look for laminar flow, helical flow, vortical flow	False lumen regurgitation fraction within 2 cm of entry tear
Vortical flow- grade 0- no vortices Grade 1- ≤ 360 degrees Grade 2- > 360 degrees	PSV in the TL, FL within 2 cm of entry tear
	Wall shear stress at the level of ascending aorta (maximum) Average axial, circumferential WSS of true lumen and false lumen at maximum size

	Percentage of energy loss from the entry tear to distal DTA with respect to entire aorta
--	--

Follow up imaging details

CT angiographic conclusions
Growth rate ≤ 5 mm/year or growth rate > 5 mm/ year
False lumen status-fully patent, partly thrombosed, completely thrombosed
Patent- contrast opacification noted completely either in arterial phase (AP) or in delayed phase (DP). Partly thrombosed- residual contrast opacification was noted in the false lumen either in AP or DP. Completely thrombosed- no contrast opacification noted due to complete thrombosis of false lumen.

APPENDIX C - PUBLICATIONS

NIL

APPENDIX D – PLAGIARISM CHECK REPORT

ORIGINALITY REPORT

10%	3%	9%	2%
SIMILARITY INDEX	INTERNET SOURCES	PUBLICATIONS	STUDENT PAPERS

PRIMARY SOURCES

1	Zachary A. Zilber, Aayush Boddu, S. Chris Malaisrie, Andrew W. Hoel et al. "Noninvasive Morphologic and Hemodynamic Evaluation of Type B Aortic Dissection: State of the Art and Future Perspectives", Radiology: Cardiothoracic Imaging, 2021 Publication	1%
2	www.ncbi.nlm.nih.gov Internet Source	1%
3	Submitted to Cranfield University Student Paper	1%
4	"Surgical Management of Aortic Pathology", Springer Science and Business Media LLC, 2019 Publication	1%